NTNU – Trondheim
Norwegian University of
Science and Technology

Structural and Petrological Study of the Klemetsaunet Plagiogranite, Trondheim, Norway

Sebastian Vedeler

Geology
Submission date: November 2013
Supervisor: Bjørn Eske Sørensen, IGB
Co-supervisor: Mai Britt Mørk, IGB

Norwegian University of Science and Technology
Department of Geology and Mineral Resources Engineering

Abstract

The Klemetsaunet plagiogranite is a felsic rock connected with the Bymarka ophiolite, and is a part of the Upper allochton of the Scandinavian Caledonides. The plagiogranitic body is cut by several mafic dikes, and this thesis provides a detailed map of the local lithologies.

The plagiogranite has porphyroblasts of garnet and hornblende that are showing syn-tectonic features. The mafic dikes have individual mineralogies, likely due to local events.

Through X-Ray Diffraction (XRD) and X-Ray Fluorescence (XRF) analyses, characteristic elements for ocean floor metamorphism are examined. The results are inconclusive, but show that regional metamorphism most likely have played a more important role than ocean floor metamorphism for the rocks in the area.

Preface

This thesis is written as a the concluding part of my Master of Science (MSc) degree in Bedrock and Resource Geology at the Department of Geology and Mineral Resource Engineering (IGB), Faculty of Engineering Science and Technology (IVT) at the Norwegian University of Science and Technology (NTNU).

I would personally like to thank my supervisors Bjørn Eske Sørensen and Mai Britt Mørk for supporting me through this process, and for the guidance they have given me along the way. Special thanks also go out to student coordinator Gerd-Inger Sætrom for assisting me with the practical sides of the thesis.

Furthermore I would like to thank all the laboratory workers who have made this work possible. Special thanks go out to Andreas Habel and the University of Stavanger for their hospitality in letting me borrow a microscope on short notice.

I would also like to express my gratitude towards fellow student Håvard Smeplass, who assisted me with field work and letting me use his camera.

Last but not least, I would like with all my heart to thank my family and friends for the support and motivation they have given me during what has been a challenging part of my life.

Table of Contents

1 Introduction

Several partially or fully intact Early Paleozoic ophiolites are located in the area around central Norway. These are part of the Upper allochton of the Scandinavian Caledonides (Slagstad 2003). Dating of these has proven two generations of ophiolites, with the larger and older group being of Late Cambrian – Early Ordovician age (Roberts, Walker et al. 2002). These are suggested formed in an oceanic supra-subduction zone and are dated to 495-475 Ma. The Bymarka ophiolite, located around Trondheim, is one of these.

Three separate plagiogranitic bodies have been linked with the Bymarka ophiolite. One of these is located at Klemetsaunet, approximately 10km west of Trondheim. Here, the plagiogranitic body is shown in a 300m sub vertical road cut along Riksvei 715 (Bynesveien). Along with the road cut, the same rocks are also exposed at the nearby shoreline, some 20m away. The crystallization age of the plagiogranite has been dated by Roberts, Walker et al. (2002) to 482±5 Ma using U-Pb dating in zircons.

The plagiogranite at Klemetsaunet is cut by several mafic dikes ranging from 1-5m in thickness. The dikes have undergone greenschist facies metamorphism, which is consistent with the rest of the Trondheim area. The plagiogranite mineralogy varies locally, and contains euhedral porphyroblasts of garnet and amphibole. It also contains calcite and several different types of mica.

1.1 Aim of Study

The aim of this study is to improve the knowledge of the processes involved in shaping the present petrology and geochemistry in the rocks at Klemetsaunet. The primary focus is put on the Klemetsaunet plagiogranite and how this rock behaves in conjunction with the penetrating mafic dikes.

Emphasis has been put on the type of metamorphism the rocks have undergone. Ocean floor metamorphism is a common alteration type for the upper parts of ophiolitic complexes. This type of metamorphism leaves a quite distinct chemical trail, as certain elements are leeched from the penetrating sea water. Investigations are done to see if this type of metamorphism has been dominant in the field area.

This thesis will provide insight of structural and geochemical details of the rocks involved, and draw a conclusion based on these data.

1.2 Regional geology

The regional geology of central Norway got attention in the late 19th century by geologists Keilhau, Kjerulf and Törnebohm (Ramberg 2008). The region is tectonically complex, characterized by massive thrust sheets from the Caledonian orogeny in late Silurian – early Devonian. There are several allocthons of rocks with different origin, and they are subjected with tectonic overprints of varying degrees (Robinson, Roberts et al. 2012). The uppermost allochton rocks originate from Laurentia, while the lower ones originate from Baltica. Following the thrusting, the region has been influenced by the extensional regime responsible for opening the Atlantic Ocean.

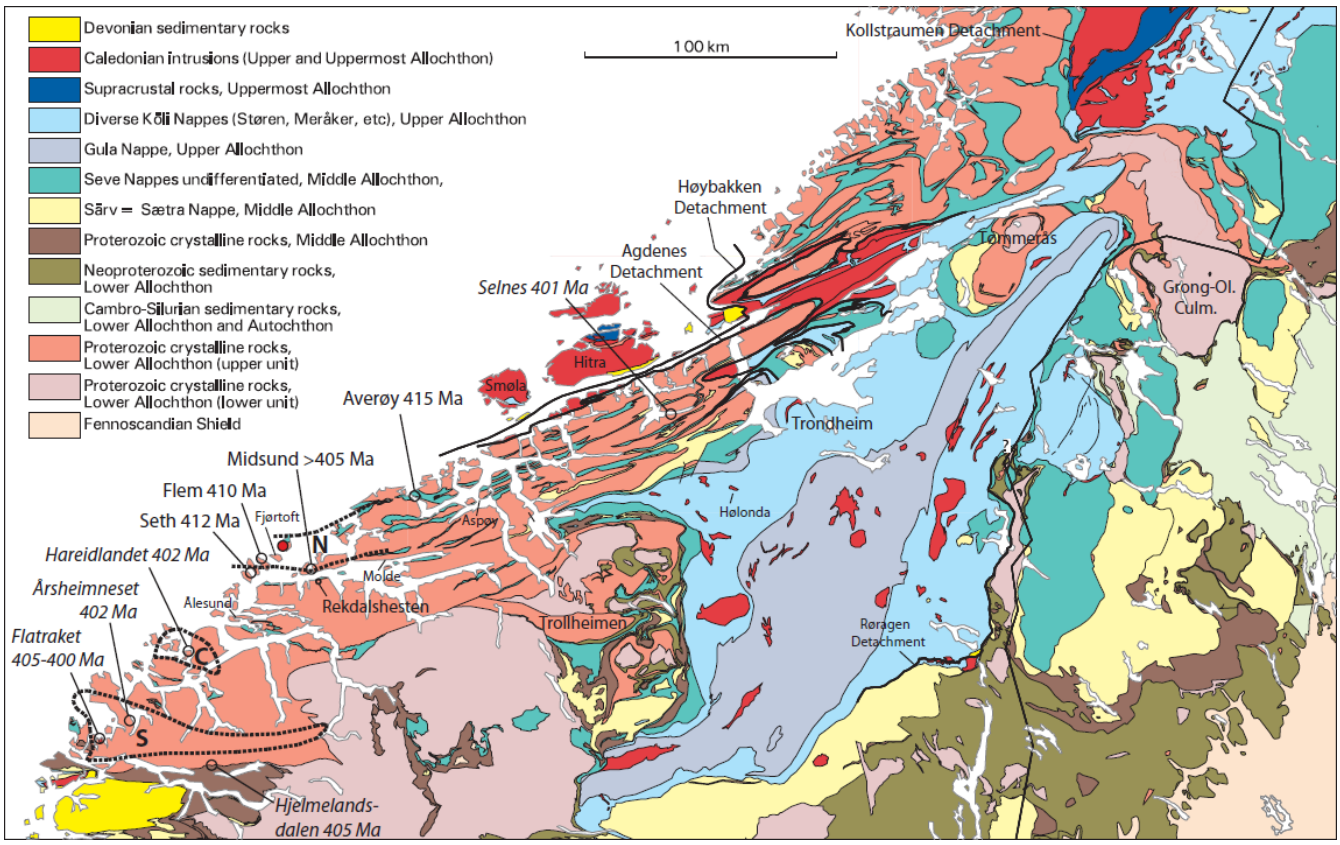

Figure 1: Map showing the complex tectonostratigraphy of mid Norway (Robinson, Roberts et al. 2012). Trondheim is located at the center of the map and the Støren nappe is marked in light blue.

The area surrounding Trondheim and its related rocks are a part of the upper allochton. The fragmented ophiolites at Bymarka along with similar ones at Vassfjellet and Løkken are a part of the Støren nappe complex (Robinson, Roberts et al. 2012). Most of the area consists of gabbros and pillow lavas, with ultramafics being rare. The ophiolites are dated to a range of 500-480 Ma, and were exhumed soon after (480-475 Ma) onto a continental margin. Biostratigraphy from overlying sediments suggest that this was on the Laurentian side of the Iapetus Ocean (Robinson, Roberts et al. 2012). The Støren nappe has many similarities with the Upper Köli nappe of north-central Sweden (Ramberg 2008).

As seen in Figure 2 and Figure 3, the area west of Trondheim mainly consists of metamorphosed oceanic basalts. However, the focus area is a small felsic pluton. The structural measurements on the map show a NNE-SSW trend, consistent with the larger scaled structures shown in Figure 1.

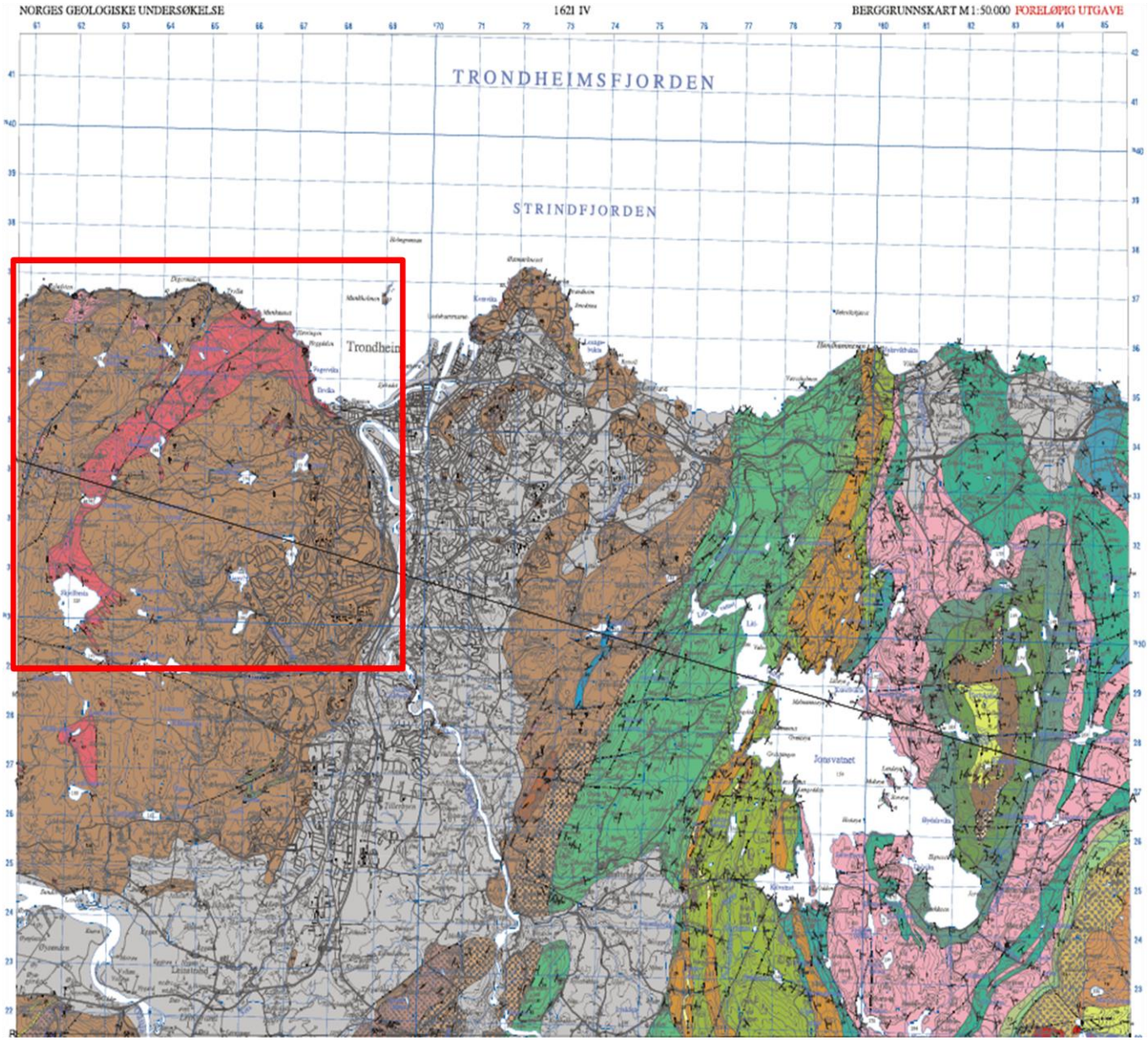

Figure 2: Geological map of Trondheim (Solli, Grenne et al. 2003). Zoom in of marked area shown in Figure 3.

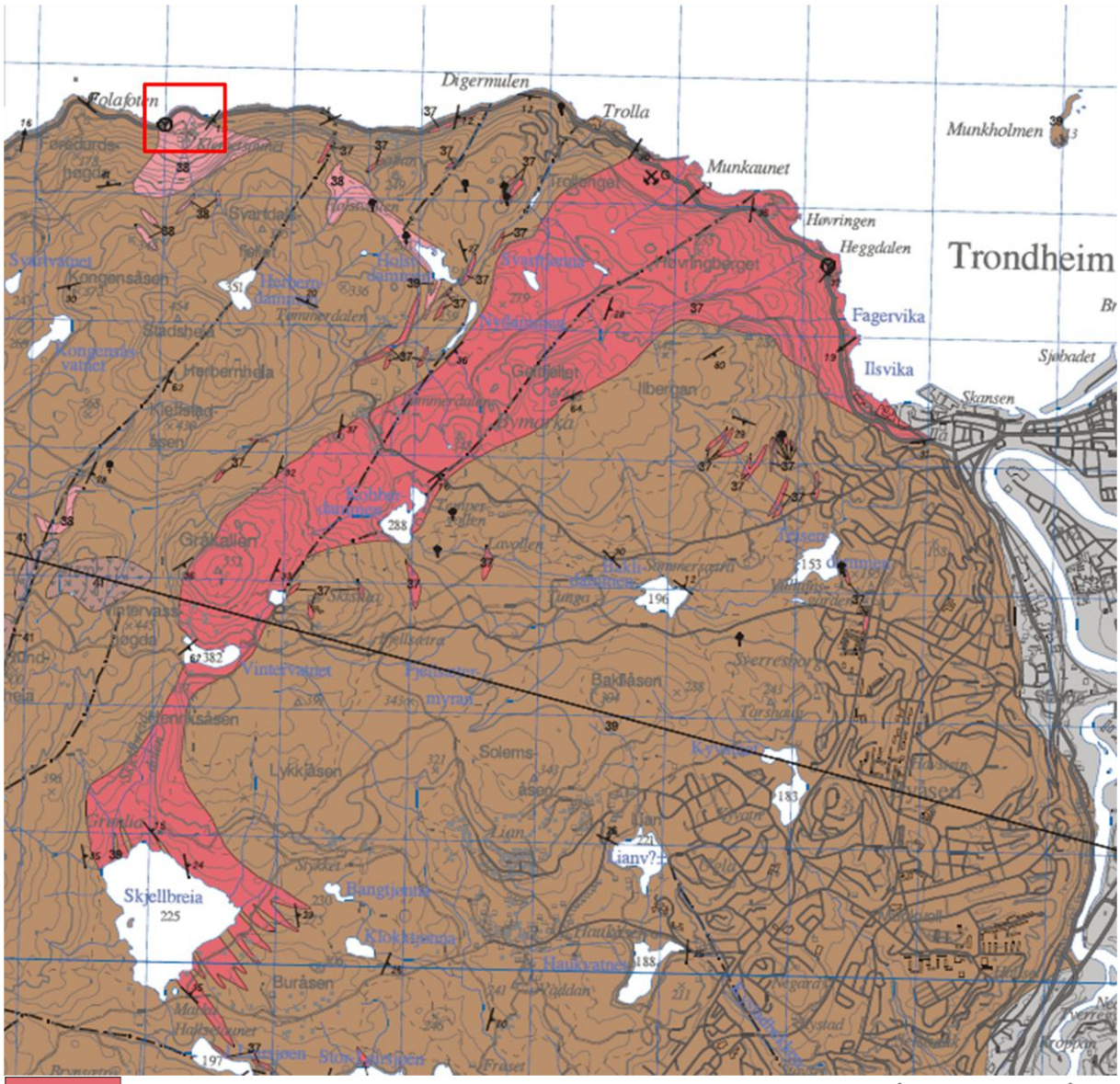

37	Trondhjemitt med overgang til granodioritt, delvis forgneiset. Ved Fagervika datert til å være ca 481 mill. år gammel *Trondhjemite with transition to granodiorite, partly gneissified. At Fagervika dated to c. 481 mill. years B.P.*
38	Kvartskeratofyr, stedvis granatførende. Opprinnelig antatt finkornige sure lavabergarter og overflatenære intrusjoner. Ved Klementsaunet datert til å være 482±5 mill år gammel *Quartz keratophyre, locally garnetiferous. Originally fine-grained acidic lavas and shallow intrusions At Klementsaunet dated to 482±5 mill. years B.P.*
39	Grønnstein (omvandlet basalt) og grønnskifer udifferensiert. Hovedsaklig putelava med lag av sur lava, kiselstein, tuffitt og diabasganger. Vanligvis deformert *Greenstone (metabasalt) and greenschist undifferentiated. Mainly pillow lava with layers of acidic lava, chert, tuffite and dolerite dykes.Usually deformed*
40	Doleritt, omvandlet, del av gangkompleks *Dolerite, metamorphosed, part of a dyke complex*
41	Gabbro, omvandlet *Gabbro, metamorphosed*

Figure 3: Zoomed in of marked area from Figure 2. The marked area on this map shows the field area of the study. (Solli, Grenne et al. 2003)

1.3 Overview of the field area

The rocks at Klemetsaunet are exposed at two main locations; a roughly 300 meter sub vertical road cut and a 100m long outcrop by the shoreline. The distance between the two exposures are about 20m, and they are separated by a road and a thin line of trees in a small hill. The correlation between the outcrops is good, but they highlight significantly different features of the rocks. This is due to the different perspective that is perceived at the two outcrops, but also due to the different local surface processes affecting them.

Figure 4: Overview of the field area with the two outcrops highlighted (outcrop at the shoreline marked in blue and road cut outcrop marked in red). (NorgeiBilder 2011).

The road cut gives a good two dimensional overview of the rocks, and sub vertical features are easy to follow throughout. It is also easy to recognize the rheological differences along the outcrop. Aside from this, the outcrop is very dusty and dirty due to the traffic along the road. Growth of liken and moss is also widespread. Clearly visible differences between felsic and mafic rock types can be hard to spot looking at the road cut from a distance. There are also weathering processes from the above lying vegetation that is discoloring the rocks along the road cut. One zone (60-70m) of the road cut is particularly contaminated by a sulphur rich vein in the rocks. Weathering of the sulphur has discolored the underlying rocks with orange, yellow and brown colors. These factors combined make it hard to get a clear perception of the color of the rocks, and also locally hides features that otherwise would be prevalent.

The shoreline outcrop gives a greater insight in the depth view that the road cut is lacking. Horizontal or sub horizontal features are easier to spot. The constant presence of sea water has also kept the rocks clean of liken and moss, and the rock colors are a lot more distinct at this outcrop, making it easier to separate the mafic and felsic rocks, as seen in Figure 5. Sea water weathering processes has however bleached rock faces, making them slightly discolored too, but not nearly as bad as most of the road cut outcrop. Closest to the seaside however, the rocks are completely covered in algae. At the shoreline outcrop it is generally a lot easier to study minerals and structural features, such as garnets or foliations, in situ, due to colors and accessibility.

Figure 5: Boundary between felsic rock (left side) and mafic dike (right side) marked with a red line at the shoreline outcrop.

A lithological map of the area was made, where felsic rock and mafic dikes are differentiated by different colors. There seems to be a decent correlation between the amount and positioning of the dikes at the shoreline and at the road cut locality. The colorless areas on the map represent places of non exposed bedrock, either due to vegetation or talus.

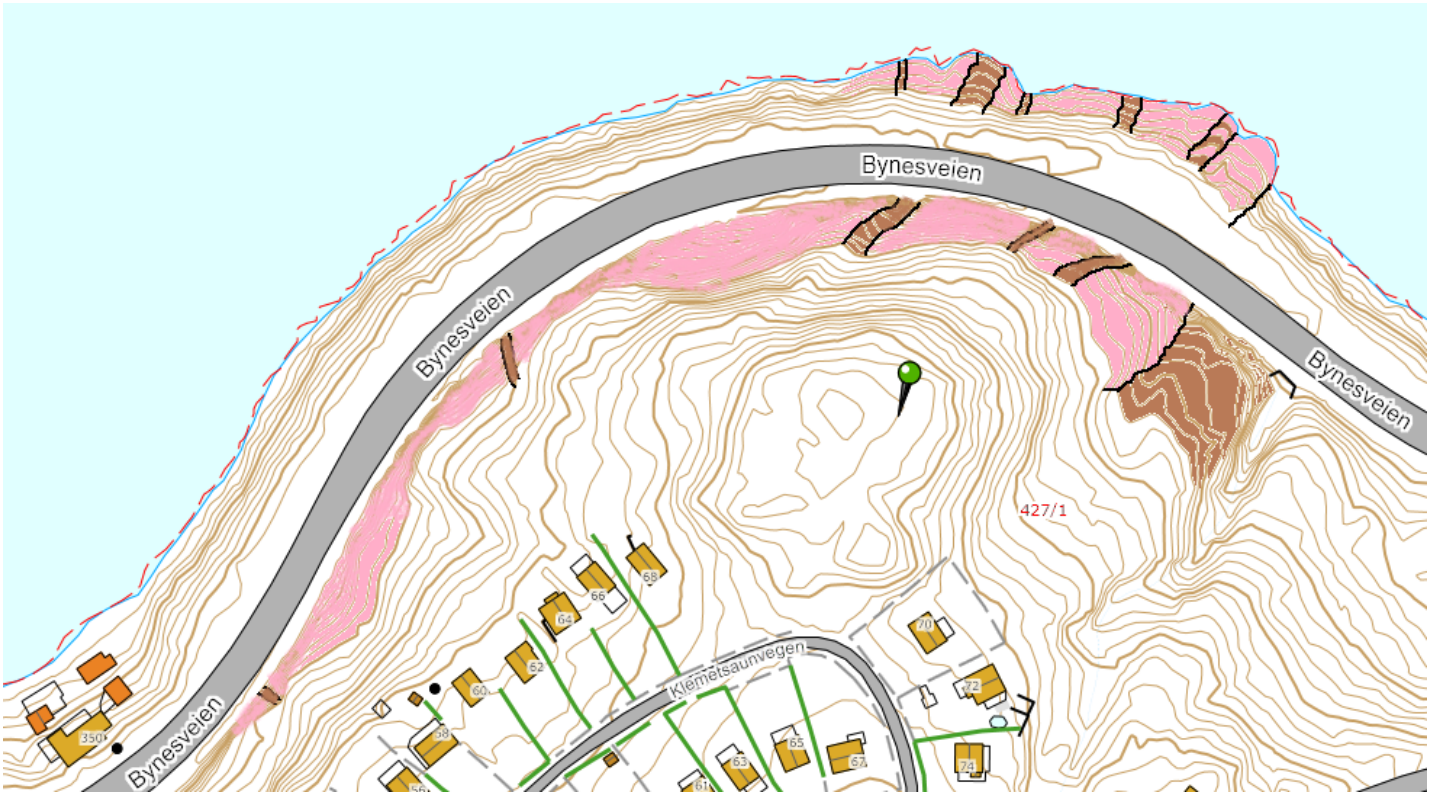

Figure 6: Map showing the lithologies of the field area. Brown = Dike, Pink = Plagiogranite. (Background map: TrondheimKommune (2013)).

1.4 Sampling strategy

At the beginning of the field work, emphasis was put on getting familiar with the field area. To support this, samples were taken to cover most parts of the outcrops. This way, large scaled general differences throughout the rocks would be revealed. Following this, a decision would be made on where to put the emphasis of a more in-depth analysis of a chosen subject.

12 initial samples (SVH1-12) were taken during the first stage of sampling, ranging over the entirety of the road cut along with one sample from the shoreline outcrop. Of these 12 samples, 9 thin sections were made, excluding some samples due to similarity with others. On the basis of these thin sections, 8 of these samples were picked for chemical analysis. 6 of these samples were felsic, and the remaining 2 were taken in separate mafic dikes.

Prior to the second stage of sampling, the decision was made to sample with specific distances from a mafic dike, to portray possible differences in the transitioning zones between felsic rock and mafic dikes. Samples were taken in the center of the mafic dike, at the border between the mafic and felsic, and 10, 30, 50, 100, and 200cm away from the dike respectively. A dike at the shoreline outcrop was chosen, on the basis of its good geographical confinement and clear geological boundaries (Figure 7).

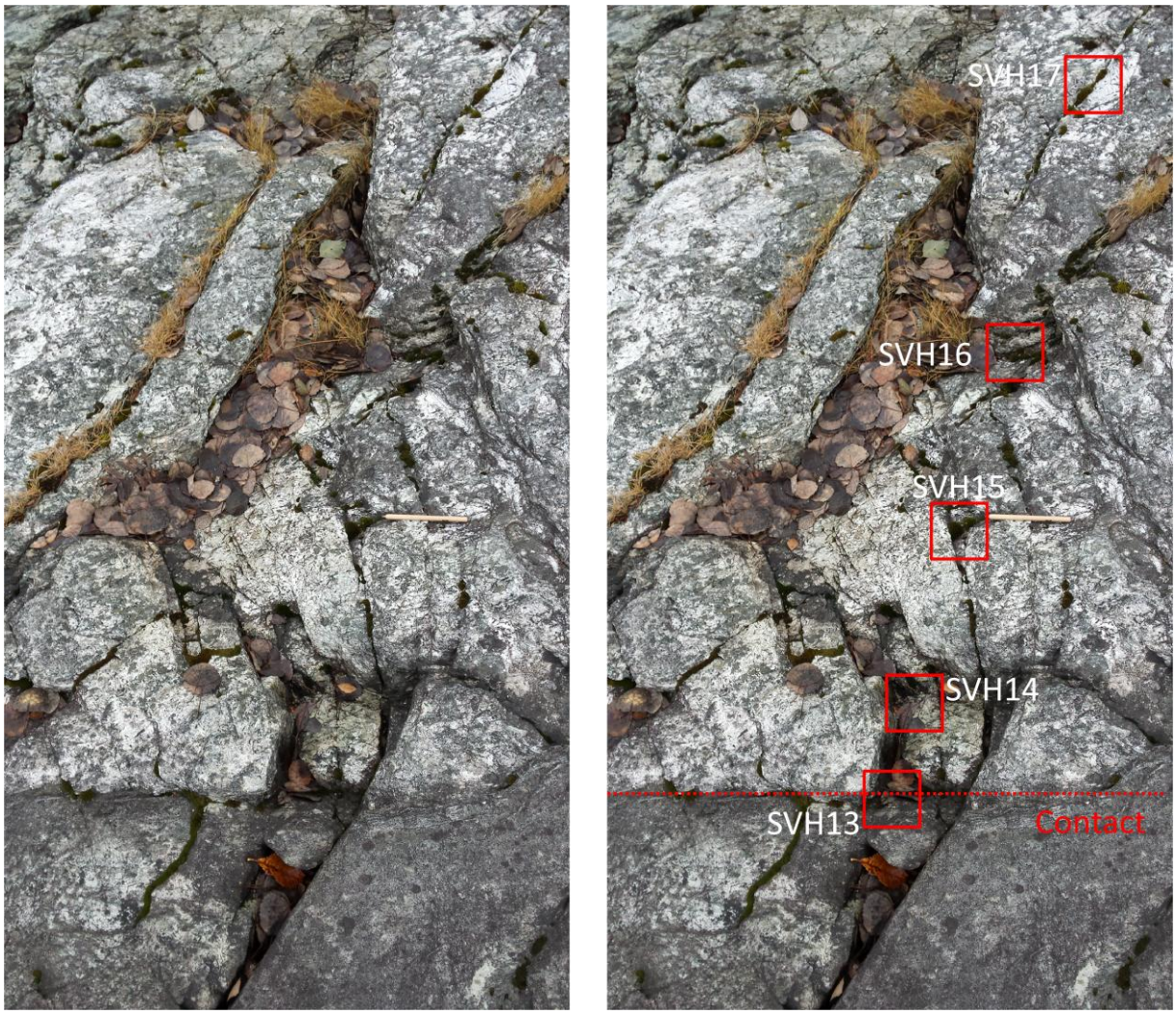

Figure 7: Sampling locations in conjunction with the dike. Along with these 5 samples, SVH18 was taken 1m further away from the dike, and SVH20 was taken in the center of the dike.

Along with these 7 samples in conjunction with the dike, a sample was also taken in a seemingly undeformed part of the felsic rock, in case they would show major differences due to deformation. Thin sections and chemical analysis were done for all these 8 samples.

For the first 8 samples, only main element XRF analysis was run. For the second batch consisting of 8 samples, both main and trace element analysis was run. The reasoning behind this is that the second set of samples was more focused on local chemical variations. Since the first set of samples was more geared towards a broader understanding of the field area, it was less crucial to get insight into the trace elements. The locations of all samples taken are shown in Figure 8.

Figure 8: Sampling locations. Picture: GoogleEarth (2012)

2 Theory

2.1 Ophiolites

Ophiolites are old oceanic crust. A complete ophiolitic complex comprises of 4 main layers (Figure 1). The uppermost layer (Layer 1) is a thin layer of pelagic sediments. Layer 2 is subdivided into 2a and 2b, being pillow lavas and sheeted dike complexes respectively. Layer 3 is a layered gabbro, further discussed below. The boundary between layer 3 and 4 is the Moho (the crust/mantle boundary). Layer 4 is composed of ultramafic rocks (Winter 2010).

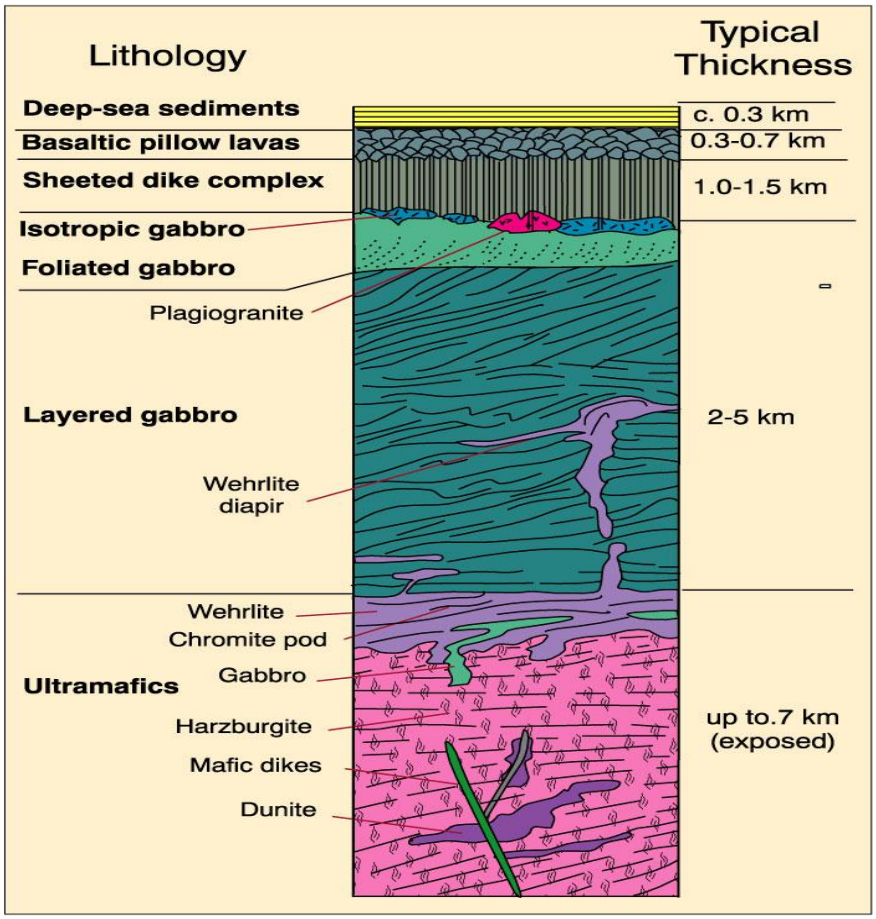

Figure 9: Diagram showing a typical ophiolite sequence with the plagiogranite at the top of layer 3 (Winter 2010).

The pillow lavas described by Robinson, Roberts et al. (2012) are a part of layer 2. However, the plagiogranite bodies as the one at Klemetsaunet are associated with Layer 3 of the ophiolite complex. These bodies are most likely generated by late fractional crystallization of the gabbroic melt (Slagstad 2003). Generally, these bodies are found in the upper part of the layered gabbros, as they rise through the gabbros after crystallization due to buoyancy (Winter 2010).

Layer 3 of the ophiolite complex is usually 2-5 km in thickness, being thinner near the oceanic ridge. The gabbro itself is formed by crystallization of the magma chamber that fed the overlying layers. Typically, the top part of the gabbro is without layering (3a), while rest (3b) shows a more distinct layering. The boundary between 3a and 3b might be obscure and is often dipping. Ultramafic bodies may also be found in the lower parts of layer 3, as they have risen from the mantle (Winter 2010), as seen in Figure 9.

2.2 Ocean floor metamorphism

The concept of ocean floor metamorphism, also called sea floor or sea bottom metamorphism was introduced in the 1960's, as a range of metamorphosed rocks with ophiolite related protoliths, like basalts, gabbros and dolerites, were found. Miyashiro (1972) summarized these findings, and generalized that the rocks typically were lacking schistosity and were metamorphosed to zeolite, greenschist or amphibolite facies. The higher grades of metamorphism occur close to the spreading ridge, where geothermal gradients are elevated.

Ocean floor metamorphism is generally speaking a type of hydrothermal metamorphosis (Winter 2010). The major characteristic of the metamorphosis is a product of the strong affiliation to seawater. The water is introduced through fractures in the rock, and is heated while seeping downwards. When the heated water rises back up due to convection, it has a stronger affinity to certain elements in the rock, and will substitute some elements for others. Miyashiro (1972) suggested that the typical geochemistry for this type of metamorphism was enrichment in Na and K, and depletion in Ca. Later studies (Coish 1977, Humphris and Thompson 1978) show that the situation is more complex, and that some elements show strong relationship with others. These elements' affinity towards enrichment or depletion in hydrothermal alteration is strongly linked with each other. A good example of this is the inverse 1:1 ratio between Mg and Ca (Humphris and Thompson 1978). The magnitude of the alteration process is also a factor of the W/R (water/rock) ratio (Lecuyer, Brouxel et al. 1990).

3 Methods

To accurately describe and investigate the petrology and geochemistry of the Klemetsaunet rocks, several analytical techniques were used along with extensive fieldwork of the study area.

3.1 Fieldwork

Fieldwork was carried out between March 2012 and November 2013. The work was supported partly by supervisors and fellow students. Dip and dip direction measurements were done with a geological compass. A handheld GPS was used to pinpoint the location of samples and pictures taken.

The topographic map used as background for the lithological map sketch was collected from TrondheimKommune (2013).

3.2 Optical microscopy

All thin sections were prepared at the NTNU thin section laboratory by technicians Arild Monsøy and Kjell Eriksen. A total of 21 thin sections were made to support this thesis. Thin sections were studied on a stereographic microscope. The microscope was used to in detail study the mineralogy, petrography and metamorphic textures of the sampled rocks. Pictures were taken with a microscope camera.

3.3 X-ray Diffraction (XRD)

The grinding of the samples was a 3-part process, and was done for the XRD and XRF (X-ray fluorescence) analyses. Initial to the crushing, hand specimens from the field were cut by saw to remove contamination from surface processes. The samples were further crushed by a Fly Press Rock Crusher. Samples that didn't obtain a desired grain size were further ground down using a Jaw Crusher with the jaw width set at 5mm. Finally, all samples were finely crushed using a tungsten carbide chamber in a Vibratory Disk Mill at 710 rotations per minute. XRD sample material was crushed for 2 minutes and XRF material for 4 minutes. As the mill only takes about 25g of sample material, a splitter was used to diminish the amount of <5mm grains before the disk mill grinding process. Using of the splitter reduces the sampling errors as it randomizes what part of the sample is kept for further grinding.

The difference grinding times for XRD and XRF samples were done to prevent the loss of crystal structure for XRD sample material. XRD sample material was further crushed in a micronizing mill for 3 minutes. 10ml of alcohol were added during this crushing. This mill is more lenient, especially towards fragile mica crystals.

The XRD samples were furthermore dried and prepared for analysis by evenly distributing the sample powder in plastic containers. XRD analysis is used to detect the crystal structure of the grain sample. This way the mineralogy of the samples is revealed. Rietveld method was also used to get quantitative analyses of the samples. The analyses were done with a Bruker D8 advance X-ray diffractometer and were interpreted by Laurentius Tijihus at the Department of Geology and Mineral Resources Engineering (IGB), NTNU.

3.4 X-ray Fluorescence (XRF)

Both main element analysis and trace element analysis were run on the XRF. For main element analysis, the sample material was weighed, and then heated to 1000°C for two hours to calculate the Loss of Ignition (LOI). 5g of the sample was then precisely weighed in along with 0,5g of flux, and put in platinum crucibles. 60µl of Lithium Iodide was added and glass pills were fused in a Claysse Fluxy. For trace element analysis, 9,6g of the crushed sample material was weighed in along with 2,4g of flux and put in a plastic container. The sample was then thoroughly mixed using a Fluxana MU-XRF Mixing set. Succeeding this, the sample pressed into a pill using a hydraulic Herzog pill press using 200kN of force for one minute.

XRF-analysis uses the fluorescing abilities of elements to distinguish and identify them. This way, elements can be both identified and quantified with XRF-analysis. The analyses were done using a Bruker S8 Tiger 4 kW X-ray spectrometer and were interpreted by Torill Sørlokk.

4 Observations

4.1 Structural geology

The plagiogranitic body is dominating the outcrops, but is cut by several mafic dikes of thicknesses 1-5m. When observed in field, the felsic rock gets noticeable more foliated near the dikes, getting an almost slaty structure next to the dikes. This also complicates rock sampling. The strikes of these dikes are all NNE-SSW, and they correlate well with the strikes and dips from Solli, Grenne et al. (2003). Dip and dip direction measurements for the mafic dikes are compiled below. These measurements show great correlation between the different dikes, as seen in Figure 10.

Dip direction	Dip
110	30
105	20
85	40
100	45
112	40
103	35
95	35
110	45
97	42
86	40
94	30
110	30

Table 1: Dip and Dip direction for the mafic dikes.

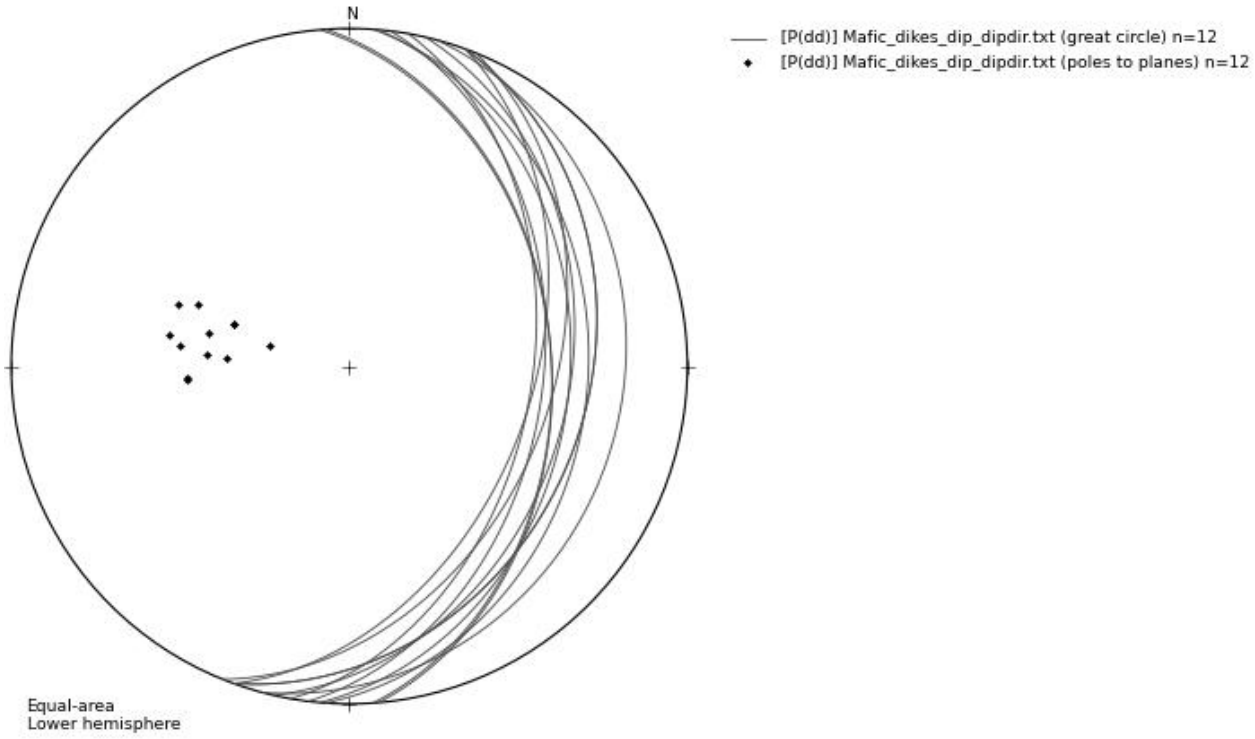

Figure 10: Stereographic projection of the mafic dikes with great circles and poles for all dip and dip direction measurements.

Hornblende crystals in the plagiogranite seem to elongate in this same N-S direction as the dikes. This could be an indication that the σ_3, the axis of least compressional stress, is perpendicular with these features. If that indeed is the case, σ_3 would be negative, meaning there has been extension along this axis (Fossen 2010). For this to be plausible, it requires that the dikes and the growth of hornblende happened at around the same time or at least during similar stress conditions. These strike measurements fit well with those taken in the layered gabbros in Bymarka (Slagstad 2003). This extensional stress field also correlates well with the regional picture post-thrusting, with the Atlantic Ocean rifting.

The eastern parts of the shoreline also show some unique structures. At this outcrop, there is evidence of a more ductile deformation not found anywhere else in the outcrops. Here, mafic and felsic parts of rock have intertwined in an almost mesh-like structure (Figure 11). The structure is very local, and seemingly diminishes or breaks off suddenly in the left part of the picture, as seen in the lower parts of the picture. The felsic rock clearly represents the majority of the two parts, and comprises of more coherent area than the mafic parts. The mafic parts consist of vein like structures seemingly breaking up the felsic parts. The general conception seems to be that most of the mafic material has a horizontal prevalence, which coincides with thinner, white veins also seen in the felsic parts.

There is reason to believe that this structure is a result of competence contrasts between the two different rock types. The mafic rock, having the relatively lowest competence, has forced itself into cracks in the felsic rock, and formed vein like structures of 5-10cm thickness, surrounding the more massive felsic parts. These competence contrasts are not to be compared with boudins, where the relative amount of the low competence phase is much higher than that of the high competence phase. The opposite of this is the case at the shoreline locality, which creates a distinctly different structure. This is the only part of the field area where such a structure is discovered, further proving the point of large local differences in deformation.

Figure 11: Intertwined felsic and mafic rocks at the eastern parts of the shoreline outcrop

In the western parts of the road cut, where the outcrop seemingly has undergone the least amount of deformation, this is illustrated well by a single, almost entirely straight vein of about 10 meters (Figure 12). The vein is light in color, and likely made of quartz, but it remains to be seen if it has the same origin and age as the thinner veins observed in the microscope. The vein observed in the rock wall is only faulted at one location with a small displacement of about 10cm, and no significant folding or deformation seems to have occurred apart from this, despite the sub horizontal fractures in the rock.

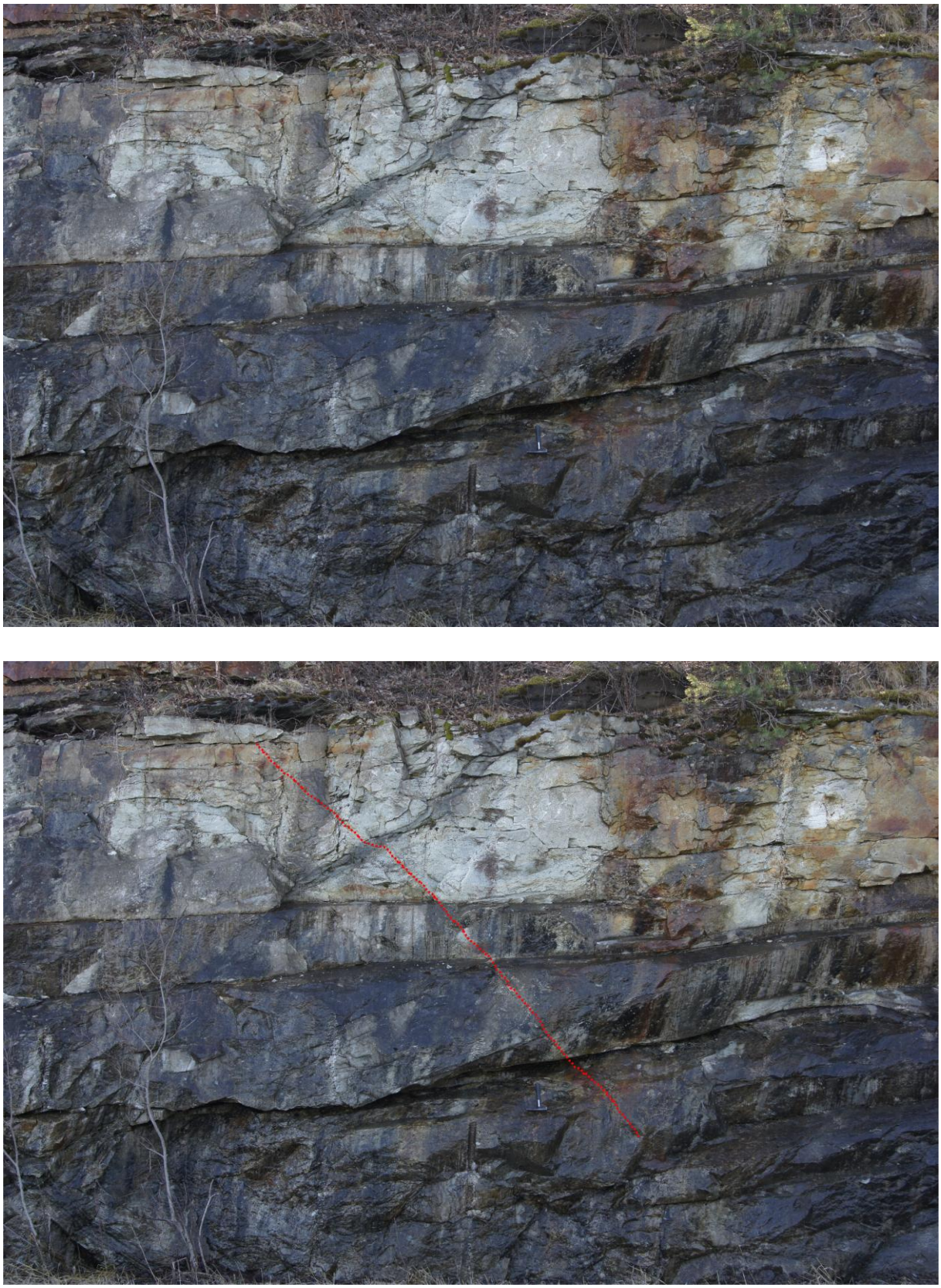

Figure 12: Single, nearly undeformed quartz vein at the road cut locality. a) And b) showing same picture. Hammer for scale located just below the vein.

4.2 Petrography, petrology and geochemistry

4.2.1 Plagiogranite

As earlier stated, the field area consists of two main lithologies. The majority of the rock mass is of felsic composition, and what is described by Slagstad (2003) as the Klemetsaunet rhyodacite. This rock is cut by several mafic dikes. The felsic rock appears in field as light to dark grey in color. At the road cut locality, the color of the felsic rock has local varieties, but these are rarely due to geological factors. The color changes coincide with the messy structural features of the road cut. These structures are heavily influenced by anthropologic work when building the road. The rock varies from massive to blocky structures seemingly random. Despite of this, some more prominent fracture planes are present.

Some mineralogical trends are also apparent on an outcrop scale. Garnets of different sizes are present along parts of the outcrop. Prismatic amphibole grains also occur over parts of the road cut, but not directly connected to the garnet occurrences. Some areas contain none of the two minerals, some areas contain only one and some areas contain both of them. The abundance of amphibole is higher in cracks or veins in the felsic rock, and there seems to be some increase in abundance when approaching the mafic dikes.

The mafic dikes at the road cut are generally darker than the felsic parts, but in some places the two are indistinguishable on an outcrop scale. The mafic rocks are dark gray to nearly black in color. Contacts between mafic and felsic rocks vary from sharp fractures to more structureless transitions. The mafic rocks show more foliated features than the felsic rocks. Some mafic parts have a slaty structure, especially notable in the eastern part of the road cut.

At the shoreline outcrop, the rock colors are more consistent. The felsic rocks have a white to light grey color. Large structural features are less prominent, but foliations are clearer than in the road cut, as seen in Figure 13. At this location, 3 different sets of foliations are easily visible. The figure also shows some interesting mineral features. Amphiboles are concentrated around the foliation marked by yellow. The foliation marked in red is likely a type of metamorphic differentiation, but this foliation is not pervasive throughout the field area. The foliation marked in green is less prominent, and seems to have a structural origin.

Figure 13 (a and b): Different foliations marked at the shoreline outcrop.

The mafic rocks at the shoreline are more consistent in color than what they are at the road cut locality. The dikes have a dark grey color, and appear significantly more massive than they do in parts of the road cut.

In hand specimens, the rock colors are more unified, both locally and between the two outcrops. The felsic rock has a light matrix color in fresh surfaces. The color is slightly lighter in the areas surrounding veins or garnets. Garnets are up to 1cm in size, and show nice crystal faces. Felsic hand specimens containing amphibole are generally slightly darker than the rest. Amphiboles are prismatic and up to 3cm in length. There are two repeating foliations throughout the felsic samples; a thin light vein and a thicker type of vein that has amphiboles growing in conjunction with it. Both vein types are bulging and do not represent flat planes.

The mafic rocks have a grey and green matrix color in hand specimens. There are also white foliation planes that are more pervasive and flatter than what is found in the felsic rock. There is a larger portion of micas in the mafic rocks compared to the felsic parts. Along with this, there are some dark minerals a few mm in size located with a persistent distance to each other.

4.2.2 Thin section analysis

The plagiogranite is composed of a matrix of small (50 - 300µm) sub/anhedral quartz and albite grains. The matrix represents between 80 and 90% of the plagiogranitic content (Figure 14). The two matrix minerals are indistinguishable in thin section microscopy, but quantitative XRD analysis showed that they have a near 1:1 ratio. Respectively, quartz and albite had an average amount of 43,9% and 44,6% of the content in the felsic samples (Table 2).

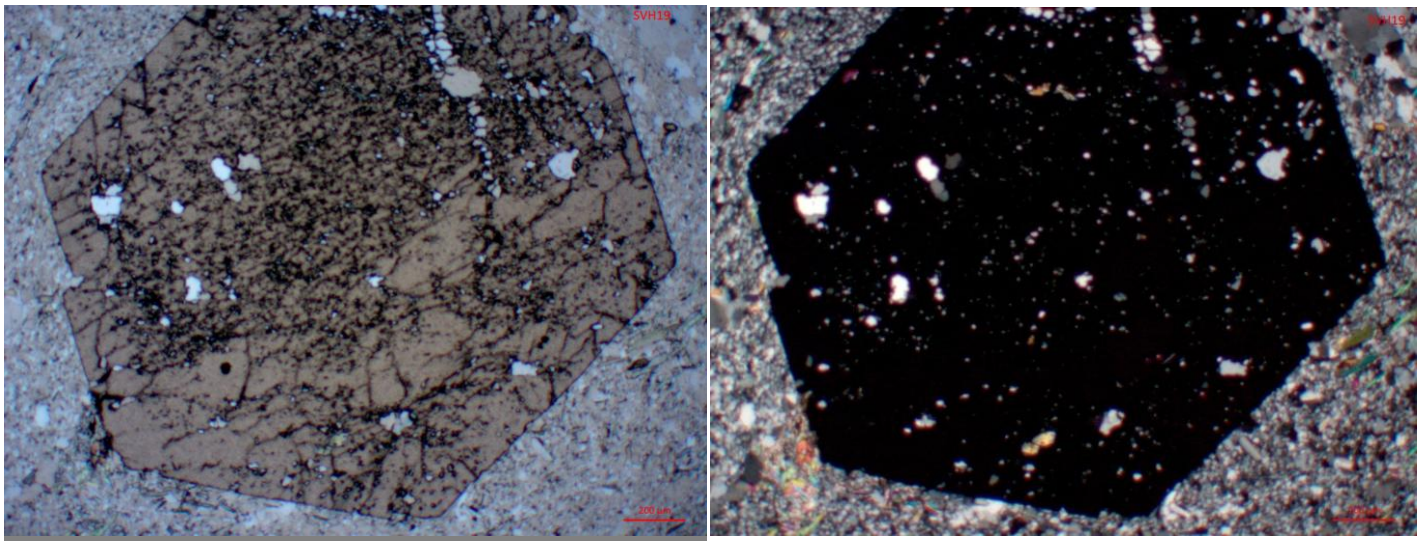

Figure 14: Euhedral garnet surrounded by matrix. a) Plane polarized light b) Cross polarized light

Sample / Mineral	SVH1	SVH2	SVH5	SVH6	SVH8	SVH9	SVH10	SVH11	SVH13	SVH14	SVH15	SVH16	SVH17	SVH18	SVH19	SVH20
Quartz	20,2	44,2	49,9	38,8	40,3	39,8	12,8	42,5	24,2	47,8	59,6	49,3	44,2	49,1	41	25,1
Albite	23,8	48,6	37,7	52	51,8	52,5	30,6	45,1	56,3	35,4	26,4	37,9	44,6	39,1	52	55
Muscovite	0,4	1,2	2,5	2,7	0,8	2,4	9,6		10,6	4,6	7,9	7,7	6,1	9,2	4,3	13
Chlorite	30,3	1,4	3,1	1,5	0,5	1,8	8,6	5,2	2,5	1,7	4,8	2	2,2	1,2		1,9
Calcite	14,7			1		1,3		0,8	1,4		1,4	1,7	1,5	1,4		1,3
Microcline	1,6	2	1,7	2,1	1,1	1,1	2	2								
Clinozoisite	9	2,7		1,8	2,5	1,8		1,6								
Hornblende			1,4		3				2,1	7,7		1,4	1,4		1,4	
Hematite						0,6										
Dolomite							36,4									
Magnesite							0,1									
Phlogopite								2,9								
Epidote									3	2,8					1,3	4,7
Total	100	100	96,3	99,9	100	101	100,1	100,1	100,1	100	100,1	100	100	100	100	101

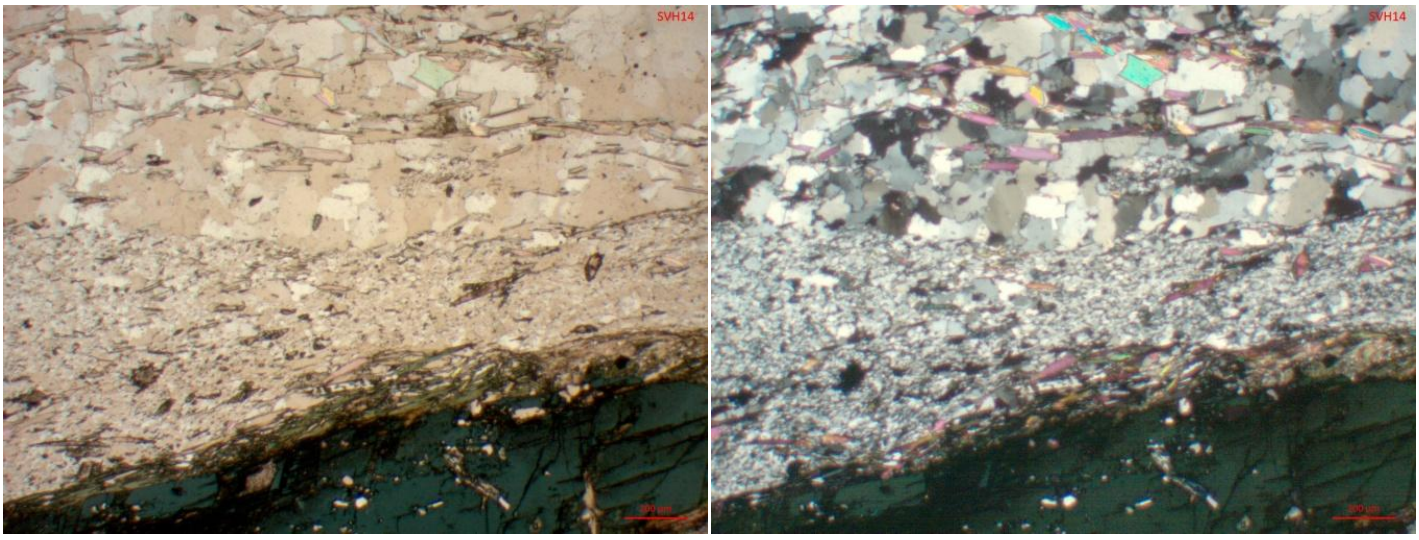

Figure 15: Thin section photo showing both intact (middle part of the photo) and recrystallized (upper part) matrix with hornblende. a) Plane polarized light b) Cross polarized light

The two matrix minerals show a varying degree of recrystallization. Parts of the plagiogranite show clear Sub-Grain Rotation (SGR) of the quartz and albite (Figure 15). In this photo, the differences between intact and recrystallized, and the grain size differences between the two become clear. Sub-grain rotation represents the second stage of dynamic recrystallization of quartz grains, following

bulging (Winter 2010). Sub-grain rotation occurs at temperatures roughly between 400-500°C. Since relatively small amounts of the matrix have undergone SGR, it is to be expected that the temperature has been in the lower part of this spectrum.

Small anhedral laths (0,1-0,2mm) of white mica are also found more scarcely throughout the matrix, as seen clearly with bright interference colors in Figure 15b. The white mica is more abundant in the recrystallized matrix, and the grains are also larger here. XRD analysis showed that this mica was muscovite. The amount of muscovite in the felsic samples varies from about 1-3%. The white mica grains are broken off, leaving signs that some degree of deformation has been present since their formation. However, as the grains in the recrystallized matrix are larger, there seems to be recrystallization ongoing in the muscovite too. Minor subhedral to anhedral biotite and chlorite grains of sizes from 0,5-1,5mm are situated more or less randomly in the matrix, but constitute for less than 1% of the felsic thin sections. There seems to be no relationship between the muscovite and other micas present in the matrix. One of the samples also showed traceable amounts (2,9%) of phlogopite on the XRD-analysis.

In some parts of the plagiogranite, large euhedral garnets (up to 5mm) are found in the matrix (Figure 14 and Figure 18). The garnets have large distances between each other, and a thin section usually only contains one large euhedral garnet, or two to three smaller subhedral ones. Garnets show inclusions of matrix minerals (quartz, albite and muscovite) with slightly smaller grain sizes to those in the matrix, and slightly rounder grain shapes than what is found in the matrix. Along with these inclusions, the garnets also devour veins of quartz. These features indicate that the origin of the garnet is metamorphic. The metamorphic growth of such porphyroblasts is limited by the diffusion of components needed for the mineral to grow. This diffusion distance limits the amount of grain that can nucleate in a rock. The growth of the garnet ceases when the diffusion distance is too large. Metamorphic growth of the garnets has left depletion haloes in the surrounding matrix, easily visible in hand specimens or in field (Figure 13 and Figure 16). The inclusions are poikiloblasts, relict matrix that has been included into the garnets as they have grown larger (Winter 2010). Poikiloblasts can also be a by-product of the garnet growth, but that is unlikely to be the main mechanism here, as the poikiloblastic minerals are depicting the surrounding rock. The round grain shape of the poikiloblasts is due to the low surface energy inside the grain compared to elsewhere (Winter 2010). This is a common way of separating poikiloblastic texture from poikilitic texture, its igneous counterpart.

The quartz veins devoured by the garnet (Figure 18) are called internal foliations (S_i), and conclude that the vein precedes the metamorphic garnet. More information can be dissected from the garnet

growth. As seen in Figure 17, the edges of the garnets show sign of rotation. This implies that the garnet is syn-tectonic, meaning that there has been ongoing deformation whilst the garnet was growing.

Figure 16: Depletion haloes surrounding garnet porphyroblasts at the shoreline outcrop

The quartz veins seen in and around the garnet are a common foliation in the rock. The veins are nearly monomineralic, and consist of larger, more recrystallized quartz grains with more developed crystal faces than what is found in the matrix. The veins have a thickness varying from 0,5-1mm, and consist of mainly subhedral grains. The abundance of the white mica in the matrix increases in and on the perimeters of these quartz veins. Along with the interaction with garnet, these veins are also broken up by micro-faulting and cut by other foliations. Relatively, the quartz veins are the oldest visible feature not related to the genesis of the rock.

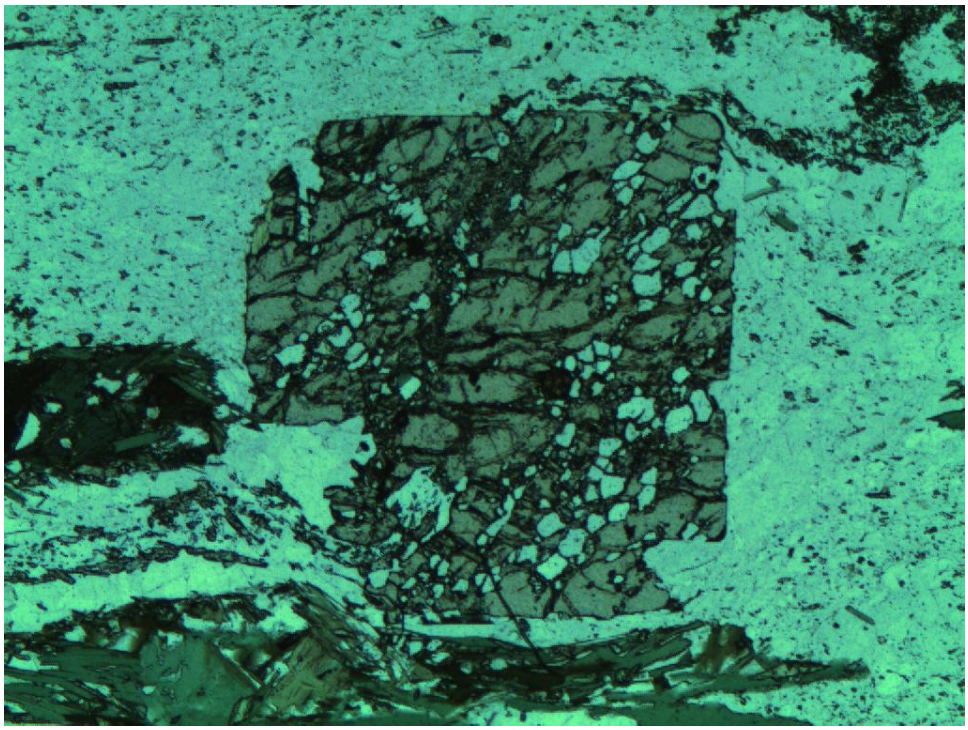

Figure 17: Garnet showing deformation with a dextral sense of shear. Plane polarized light.

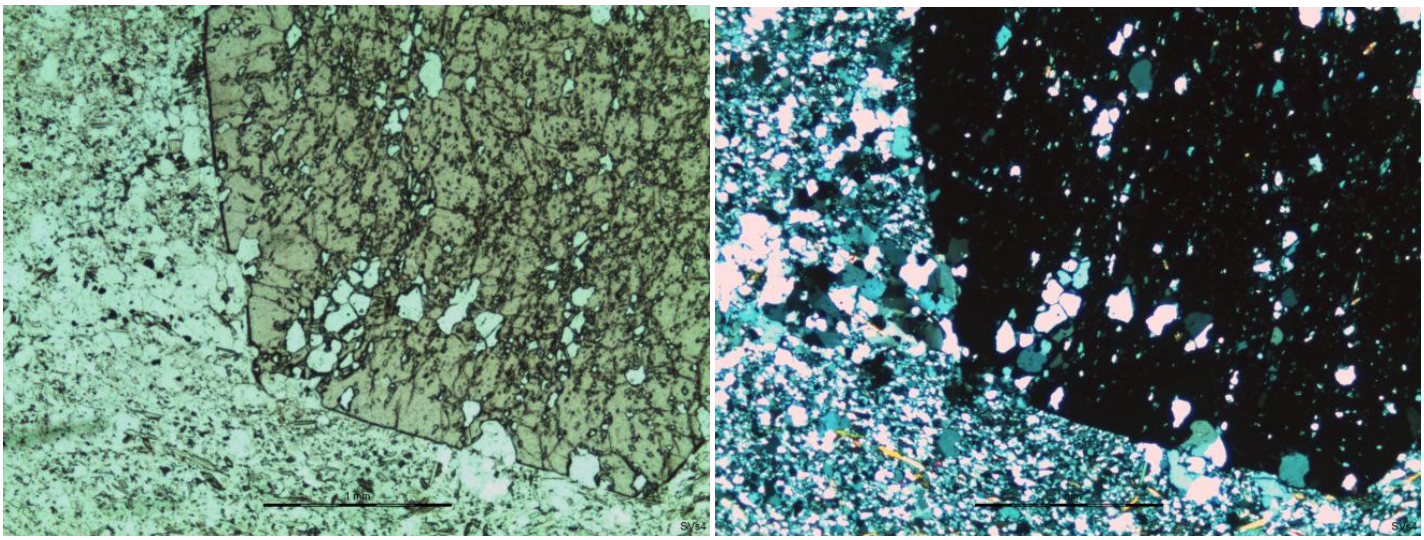

Figure 18: Poikiloblastic texture with quartz inside a garnet porphyroblast. A vein of quartz is coming in from the left and is devoured by the garnet. a) Plane polarized light. b) Cross polarized light

In addition to the quartz veins, there are also larger foliations (thicknesses around 3-5mm) with more mafic contents in the certain parts of the plagiogranite. These foliations generally contain some large (up to 3,5mm), prismatic grains of hornblende surrounded by larger amounts of chlorite and some biotite. Similar to the garnet, the hornblende also contains porphyroblasts of matrix minerals (Figure 19).

The biotite grains in conjunction to the foliations are noticeably more lath-shaped than the ones scattered in the matrix, and have a length of up to 1,5mm. Chlorite grains are subhedral with sizes around 1mm. Where these veins are thinner, there is also less hornblende and more of these micas. There are also larger euhedral grains of white mica (up to 1,5mm) hugging these veins, seemingly formed as a reaction between the foliation and the host rock.

The hornblende foliations cut the quartz veins, and are therefore considered as the younger feature of the two. This, along with the poikiloblasts found in the hornblende, implies that these veins are a feature non-related to the forming of the rock. Contrary to the garnet, the hornblende grains do not show clear signs of deformation. However, it is natural to assume that the hornblende growth is metamorphic, as the poikiloblasts resembles the matrix content so well.

In these veins, there are certain places where biotite and chlorite are filling what clearly are relict grains of hornblende (Figure 19). The outline of the hornblende grains are still there, but the mineralogy has been altered. This metamorphic alteration in mineralogy represents a dip in pressure and temperature, and is a product of retrograde metamorphism. As this occurred after peak metamorphism, this is expected to be one of the youngest features easily visible in the plagiogranite. Figure 20 shows that there also are transition zones between hornblende and chlorite, further confirming that these grain shapes of biotite and chlorite indeed are pseudomorphs after hornblende. This suggests that the retrograde metamorphism is ongoing.

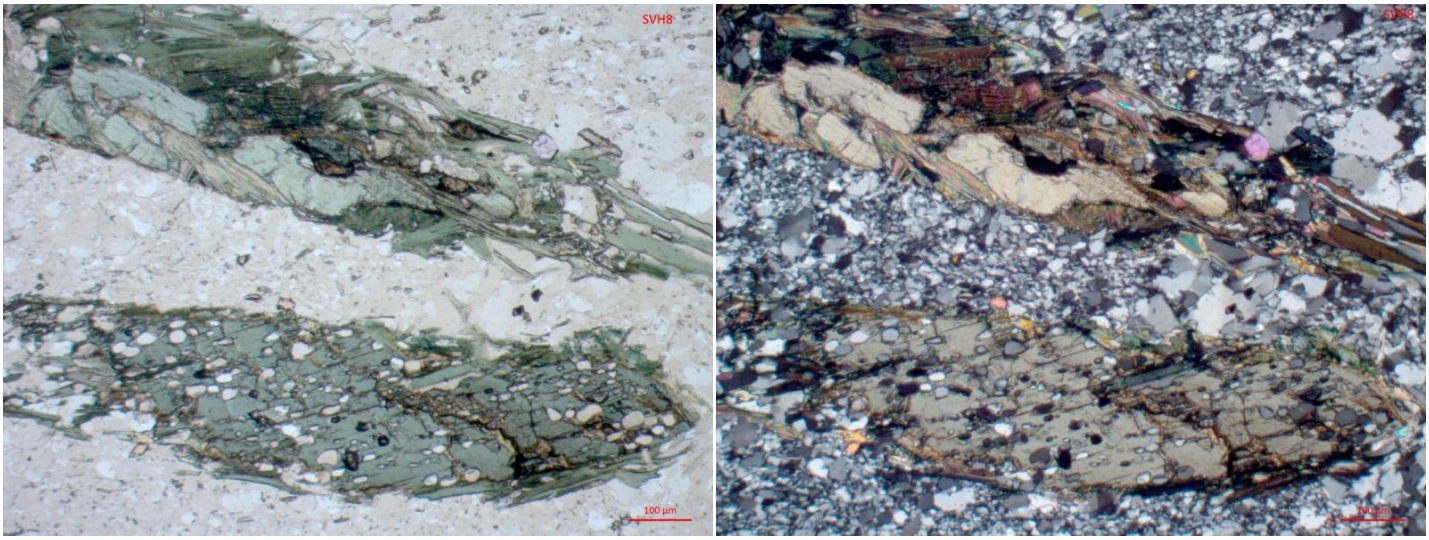

Figure 19: Replacement of hornblende by biotite and chlorite. Upper grain is replaced by chlorite and biotite, while the lower grain is nearly intact hornblende. a) Plane polarized light. b) Cross polarized light

The abundance of the hornblende veins seems to be related to nearby mafic dikes and it also seems to have some effect on the content. The most interesting observation is the alteration of hornblende.

In association with the amphibole bearing foliations, there are quite a lot of opaque minerals. Most of the opaque minerals have are euhedral with a cubic crystal structure, while a smaller number are subhedral. Two of the opaque mineral phases are confirmed as pyrite and chalcopyrite using reflected light on the polarization microscope. The opaques are most commonly seen inside or near the hornblende, but smaller grains also occur seemingly randomly in the matrix.

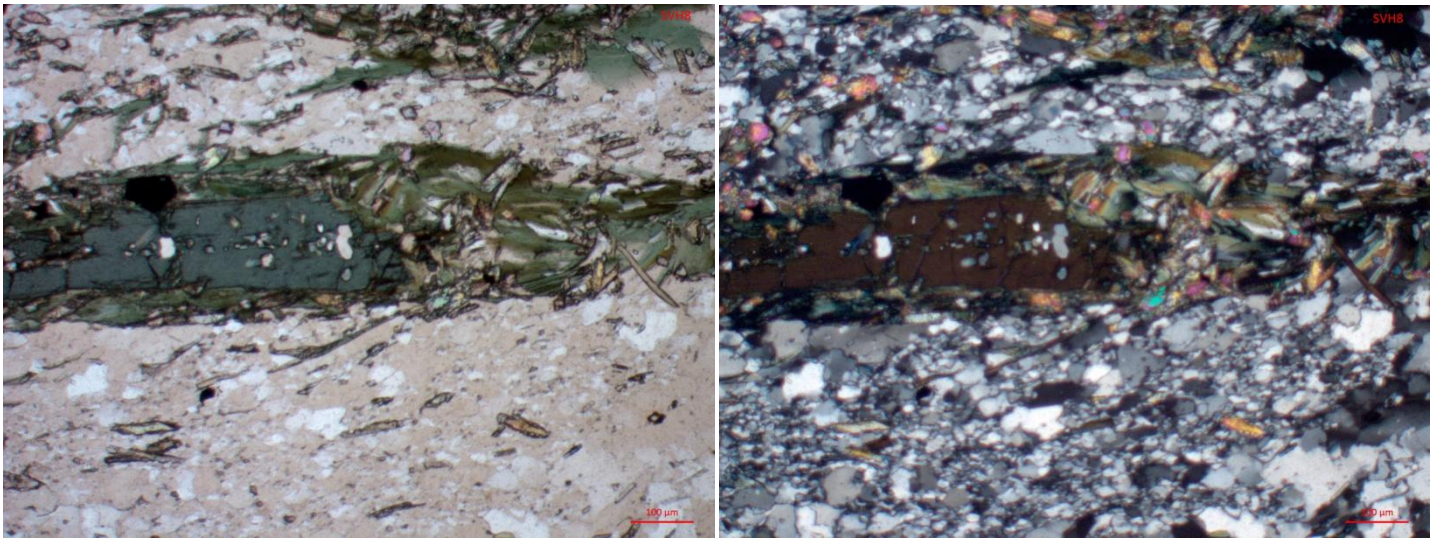

Figure 20: A hornblende grain that is undergoing alteration to chlorite. a) Plane polarized light. b) Cross polarized light.

4.2.3 Mafic dikes

While the plagiogranite in the area has a reasonably homogenous mineral content, the mafic dikes have more local variations in the mineralogy. The general trend is that there is that the rock has undergone some variation of greenschist facies metamorphism. The 3 different mafic dikes sampled had quite diverging results. However, some similarities were apparent; Chlorite is found in every sampled mafic dike, although in varying quantity. Carbonate minerals were also found in all mafic samples, although one of the dikes contains dolomite and the other two contain calcite. Euhedral epidote was also present in all 3 sampled dikes, narrowing the facies down to epidote greenschist. A similar mineralogy is discussed in Gerlach, Leeman et al. (1981), also describing altered oceanic basalts in the vicinity of plagiogranites.

The first sampled dike (SVH1) is slaty in hand specimen and has the look of a typical greenschist. It has a very high chlorite (30,3%) content compared to the other mafic samples, and as seen in Figure 21, the chlorite behaves like a matrix of intergrown laths, binding the rock together. Along with the chlorite, the standard quart and albite matrix is still present, however with a less prominent role, and

more recrystallized than what is generally seen in the felsic rock in the area. Along with these minerals, the dike also contains equal amounts of calcite and euhedral epidote.

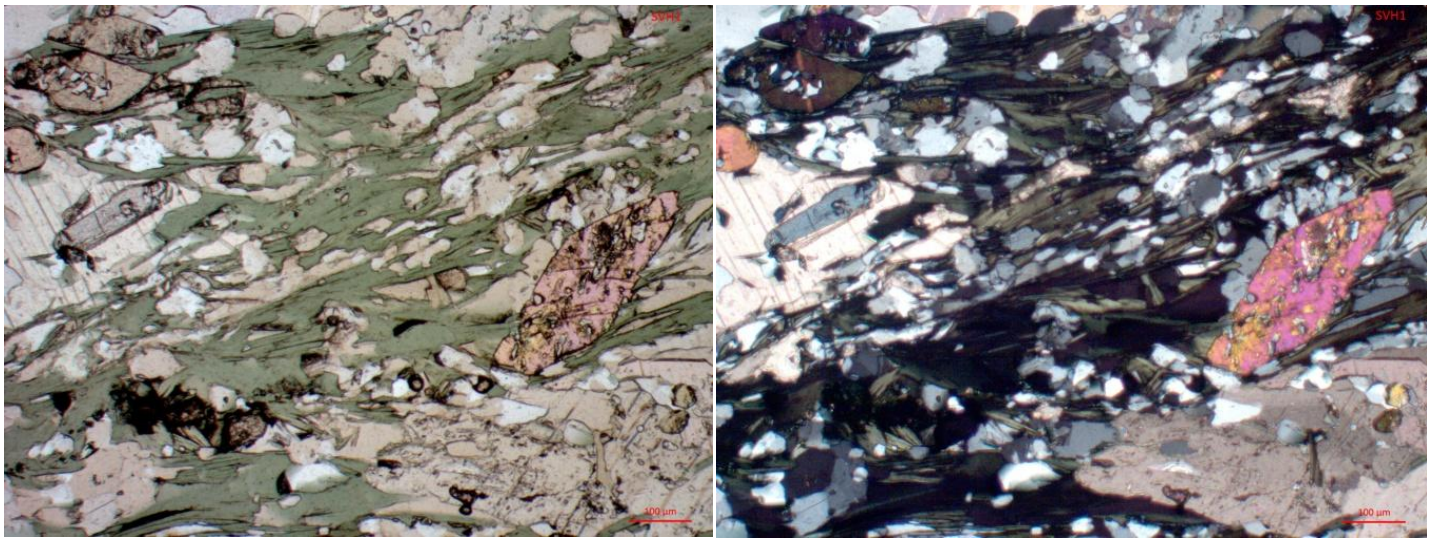

Figure 21: Mafic dike (SVH1) containing mainly chlorite, quartz+albite matrix, calcite and epidote

The second mafic dike that was sampled (SVH10), located about 150 meters west of the first one, has a mineralogy characterized by large amounts of dolomite (Figure 22). This was distinguished from calcite by XRD analysis. Along with the dolomite, chlorite is also present in the sample. The chlorite content is less in SVH10, and the chlorite is also less deformed. The slaty texture of SVH1 is not present in this sample, but the mica grains seem to have a preferred orientation. Additional contents include quartz and albite matrix, muscovite and small amounts of epidote.

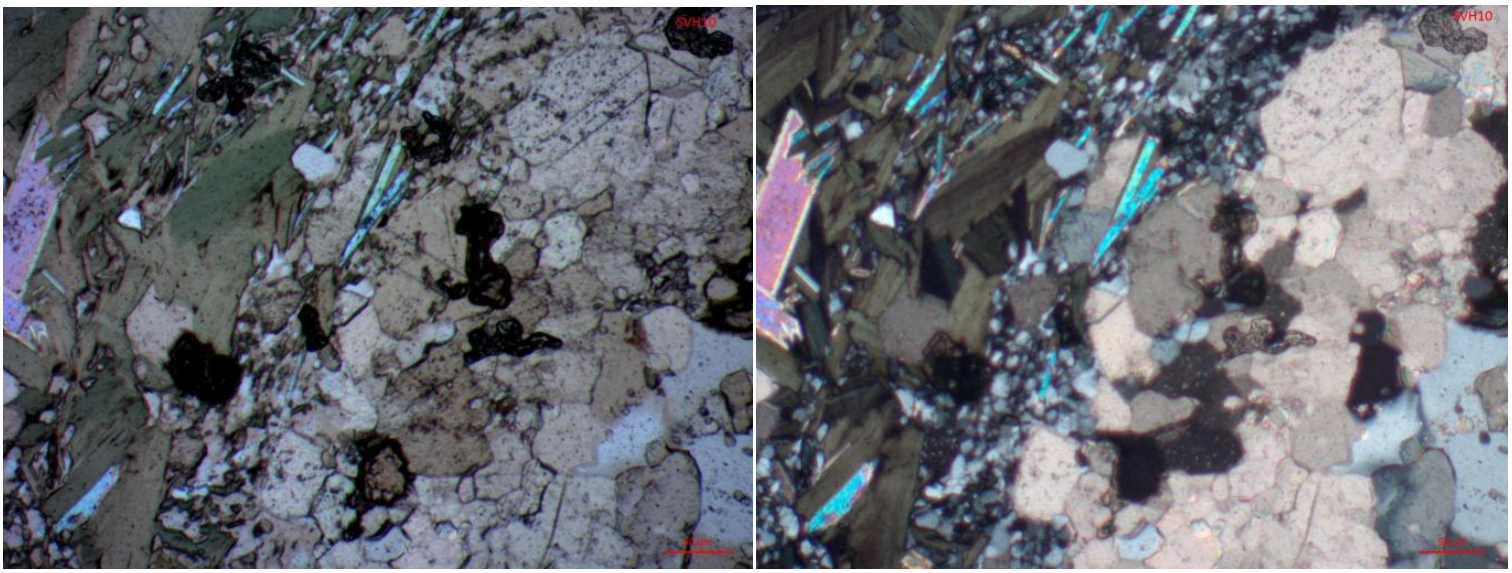

Figure 22: Mafic dike (SVH10) containing large amounts of dolomite, along with chlorite and quartz+albite matrix and muscovite.

The contents of the last sampled dike (SVH20), has a much larger fraction of quartz and albite matrix than the others. The mineralogy of this dike is not far from that seen in the felsic parts, but differs with the contents of euhedral epidote. Additionally, the matrix content is in the lower spectrum of what we find in the felsic rocks. The sample has a SiO_2 content of 67,6% (Table 3), which by definition makes it an intermediate rock. It's also notable that SVH20 had the highest muscovite content of all the sampled rocks. In SVH13, the sample located at the contact between this dike and the plagiogranite, hornblende is also present. However no hornblende or other amphiboles are found in any of the three sampled dikes, neither in thin section nor XRD analyses.

Along with the carbonates present in the dikes, there are small amounts of calcite of varying size (0,2-0,5mm) present both in the matrix of the felsic rock. The calcite grains show thick tabular calcite twins, which can be used as a temperature gauge (Figure 23) (Ferrill, Morris et al. 2004). This study shows that thick twins like the ones seen mainly in the mafic dikes at Klemetsaunet generally form at temperatures of 300°C and above.

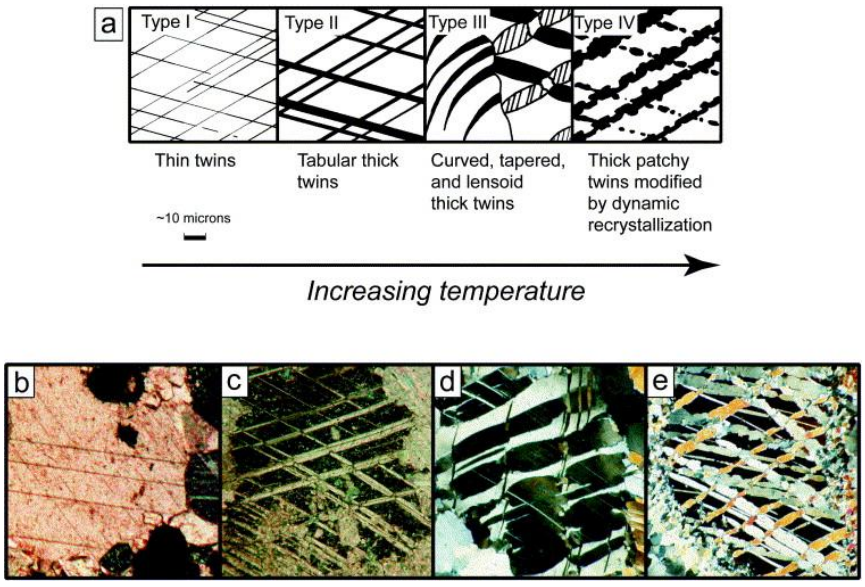

Figure 23: Temperature influence on calcite twinning (Ferrill, Morris et al. 2004)

4.2.4 Nomenclature

The felsic rock at Klemetsaunet has been given several names. The general term plagiogranite can be used, but is a general suite of rocks and not a specific rock name. Plagiogranites include diorites, trondhjemites and tonalities among others (Grimes, Ushikubo et al. 2013). They are characterized chemically by high SiO_2 and low K_2O values (Gerlach, Leeman et al. 1981), and are the counterpart to peralkaline granites.

Regional maps of the area published by NGU (Norwegian Geological Survey) have named the felsic rock quartz keratophyre. While this is a more precise term than plagiogranite, the term still grasps a series of rocks rather than a single petrographic rock type. A keratophyre is a collective term for albitized leucocratic Na-rich volcanic rocks (Schermerhorn 1973).

Roberts, Walker et al. (2002) and (Slagstad 2003) calls the rock a rhyodacite, although specifying that the rock indeed has undergone metamorphism, even though they gave it an igneous name. A rhyodacite is a rock that falls close to the border between the rhyolite and dacite (3b and 4) fields in the QAPF diagram for volcanic rocks (Figure 24) (Streckeisen 1980).

In this thesis, the rock is consistently called a plagiogranite or oceanic plagiogranite. While rhyodacite is a more specific term for the rock content, the tern oceanic plagiogranite gives a better understanding of the rock's origin.

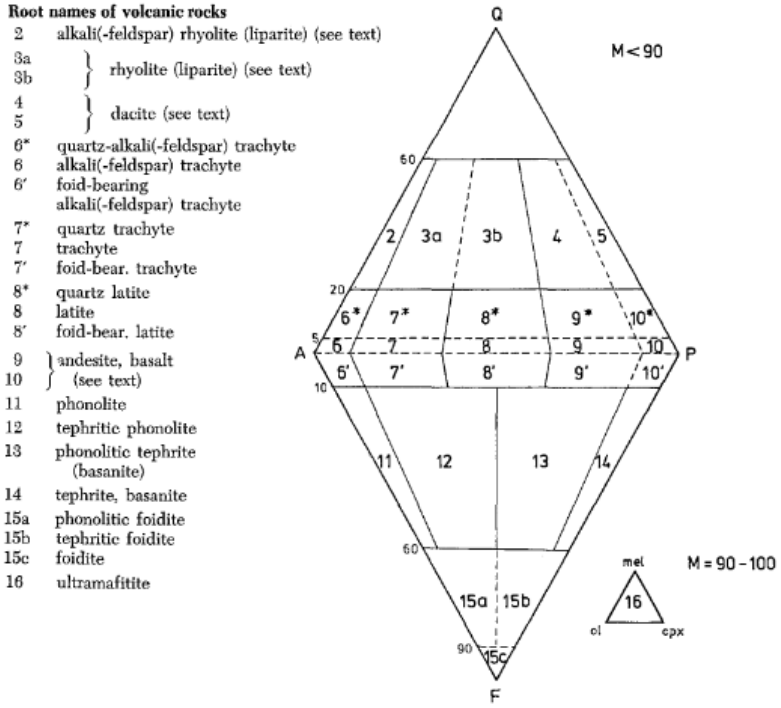

Figure 24: QAPF diagram for volcanic rocks(Streckeisen 1980).

4.2.5 Geochemical analysis

The results from the XRF analyses are presented in table 3 and 4.

Sample / Element	SVH1	SVH2	SVH5	SVH6	SVH8	SVH9	SVH10	SVH11	SVH 13	SVH 14	SVH 15	SVH 16	SVH 17	SVH 18	SVH 19	SVH 20
Fe2O3 (%)	11,61	1,92	3,02	2,65	1,66	3,06	10,02	3,97	3,04	3,33	5,30	2,56	3,02	3,53	1,90	2,73
TiO2 (%)	1,12	0,16	0,15	0,16	0,14	0,16	0,97	0,17	0,31	0,15	0,14	0,14	0,14	0,16	0,15	0,34
CaO (%)	10,51	0,78	1,28	0,57	1,20	1,01	10,89	0,58	1,32	1,40	0,92	0,88	0,49	0,30	0,53	3,33
K2O (%)	0,09	0,26	0,55	0,49	0,08	0,34	1,50	0,37	1,35	0,58	1,04	0,43	0,39	1,18	0,52	1,61
P2O5 (%)	0,10	0,02	0,02	0,01	0,03	0,01	0,10	0,01	0,11	0,00	0,01	0,01	0,01	0,01	0,01	0,10
SiO2 (%)	48,43	77,03	76,40	75,44	76,63	74,35	48,51	74,37	68,89	76,83	77,44	79,88	77,90	75,79	77,25	67,57
Al2O3 (%)	15,74	11,28	11,18	12,33	11,95	12,14	14,22	11,96	16,94	11,16	10,13	10,09	11,40	11,42	12,52	17,01
MgO (%)	7,87	0,20	0,95	0,12	0,26	0,28	7,71	1,11	0,71	0,71	1,20	0,55	0,55	0,44	0,11	0,76
Na2O (%)	2,71	5,89	4,64	6,58	6,40	6,51	4,28	5,68	7,00	4,37	2,94	4,59	5,67	4,63	6,35	6,27
MnO (%)	0,25	0,03	0,05	0,05	0,03	0,04	0,31	0,07	0,04	0,05	0,05	0,05	0,05	0,02	0,03	0,05
Sum (%)	98,43	97,55	98,23	98,40	98,38	97,89	98,51	98,29	99,71	98,58	99,17	99,18	99,61	97,49	99,37	99,77
LOI (%) 850°C	9,96	0,62	0,92	0,46	0,42	1,04	15,15	1,21	1,28	0,78	2,03	1,06	0,81	0,90	0,43	3,07

Table 3: Results from XRF main element analysis

The samples analyzed are divided into three sub groups. Group 1 is the mafic dikes. This group consists of samples SVH1 and SVH10, and is marked brown in the result tables. Group 2 is the felsic samples that are taken not in relation with a dike. This group consists of samples SVH2, SVH5, SVH6, SVH8, SVH11 and SVH19, and is marked pink in the result tables. Group 3 consists of all samples taken in relations to a dike. This comprises samples SVH13-18 and SVH20, which are marked blue on the result tables.

The samples in group 3 have varying degree of silica content. Sample SVH20 and SVH13 are intermediate in composition, and are taken in the center of the dike and on the boundary of the dike, respectively. This is, as previously mentioned, the only sampled dike which is not mafic in composition. The rest of the samples in group 3 (SVH14-18) are taken with increasing distance away from the dike, and are felsic in composition. When commenting on felsic samples in general, these five samples will be included along with the samples in group 2.

The plagiogranite ranges in SiO_2 content from 74-80%, which is well within the limit for felsic rocks at >69%. The iron (Fe_2O_3) content varies between 1,6% and 5,3%, and is largely a factor of the difference in abundance of hornblende and sulphides in the samples. SVH15, which has the highest Fe_2O_3 content with well over 1% discrepancy to the next sample, has visibly more of these minerals than the rest. Other main elements like Aluminum, Titanium, Phosphor and Manganese all show quite stable values throughout the felsic samples. Samples SVH6, SVH8, SVH9 and SVH19 show slightly higher Al_2O_3 contents than the remaining felsic samples, but this correlates well with the ratio between albite and quartz. The four aforementioned samples all have an albite content of >50% (Table 2), while none of the other samples show the same.

If the rock had undergone hydrothermal alteration, one would expect to see a notable enrichment in Potassium and Sodium if this is the case (Miyashiro 1972). Additionally, an inverse 1:1 relationship between enrichment of Magnesium and depletion of Calcium would be expected from hydrothermal alteration (Humphris and Thompson 1978). To investigate this, one needs to evaluate if the values of these elements change consistently when approaching a dike. As the dikes represent paleo-weakness planes, they represent the most likely conduit for hydrothermal fluids and succeeding alteration.

Sample Element	SVH 13	SVH 14	SVH 15	SVH 16	SVH 17	SVH 18	SVH 19	SVH 20
Sc (PPM)	3	2	4	2	1	4	2	3
TiO2 (%)	0,31	0,149	0,137	0,137	0,138	0,156	0,14	0,324
V (PPM)	20	9	6	4	4	6	6	31
Cr (PPM)								
MnO (%)	0,037	0,046	0,049	0,05	0,046	0,021	0,025	0,052
Fe2O3 (%)	2,717	3,222	4,825	2,215	2,59	3,061	1,549	2,353
Co (PPM)	97	130	108	103	98	104	114	53
Ni (PPM)	6	8	8	4	6	7	5	5
Cu (PPM)	3	9	17	2	5	3	1	4
Zn (PPM)	97	119	182	72	83	77	49	50
Ga (PPM)	25	20	24	17	19	26	23	19
As (PPM)	16	26	20	17	17	18	19	9
Rb (PPM)	26	11	20	9	7	18	7	31
Sr (PPM)	244	185	169	69	62	62	55	527
Y (PPM)	23	112	75	74	82	92	96	7
Zr (PPM)	100	291	273	277	277	314	284	93
Nb (PPM)	8	6	7	6	6	9	8	5
Mo (PPM)	1							
Sn (PPM)			1	1	1	3	3	
Sb (PPM)	5	5	5	5	6	4	6	7
Cs (PPM)	1	1						
Ba (PPM)	312	116	197	79	58	162	57	341
La (PPM)	4	3			9	7	2	
Ce (PPM)	14	48	33	29	50	39	56	15
Pb (PPM)	7	7	19	3	4	4	5	15
Th (PPM)	3	2	2	1	1	1	2	3
U (PPM)	1							1

Table 4: Results from XRF trace element analysis

Trace element XRF analyses show good correlation with the main element analyses in regards to the TiO_2, Fe_2O_3 and MnO values. The analyses for the group 3 samples also show some systematic differences in regards to where the samples were taken.

In the main element XRF analysis the sample taken in the intermediate dike (SVH20) and the sample at the contact of this dike (SVH13) show very similar values for most elements. However, for the trace element values, we see that these two samples differ quite a lot for certain elements. This is likely a result of enrichments of some elements in minerals that precipitate at the contact between the two lithologies.

Humphris and Thompson (1978) tested the mobility of certain trace elements in oceanic basalts during hydrothermal alteration. This was done by comparing sampled altered rock values to standard values for fresh basalts. When comparing against the standard values used in this study, it is important to note that they applied values for basalts located at a relatively higher point in the ophiolite sequence, and that the sea water penetrating at the shallow depth will have a larger elemental substitute potential.

5 Discussion

One of the sampled dikes contains large quantities of dolomite (Table 2). Carbonates are common in the mineralogy of the rocks in the area, but this is the only sample which shows a magnesium carbonate. As Mg is one of the elements that is enriched in ocean floor metamorphosed rock (Miyashiro 1972, Coish 1977), this process could be a possible explanation for this mineralization. The magnesium from the dolomite could possibly originate from sea water; however that would prove peculiar because of the lack of dolomite in the adjacent dikes. The source for the magnesium should rather be interpreted as a more local enrichment or event.

Ocean floor metamorphism causes enrichment of K and Na via leeching of the sea water (Miyashiro 1972). As previously stated, hydrothermal alteration of the rocks using the dikes as fluid conduits should give the plagiogranite lower values of the hydrothermally enriched elements the further you move away from the dike. This is illustrated by graphs for the separate elements in question.

The Sodium content in relations to the distance from the dike (Figure 25) seems to have little consistency. There is a general trend of a decreasing value away from the dike, but the results are not unequivocal. For the Potassium content (Figure 26), the results are also diverging. Similar to the K_2O values, there is a general decreasing trend away from the dike.

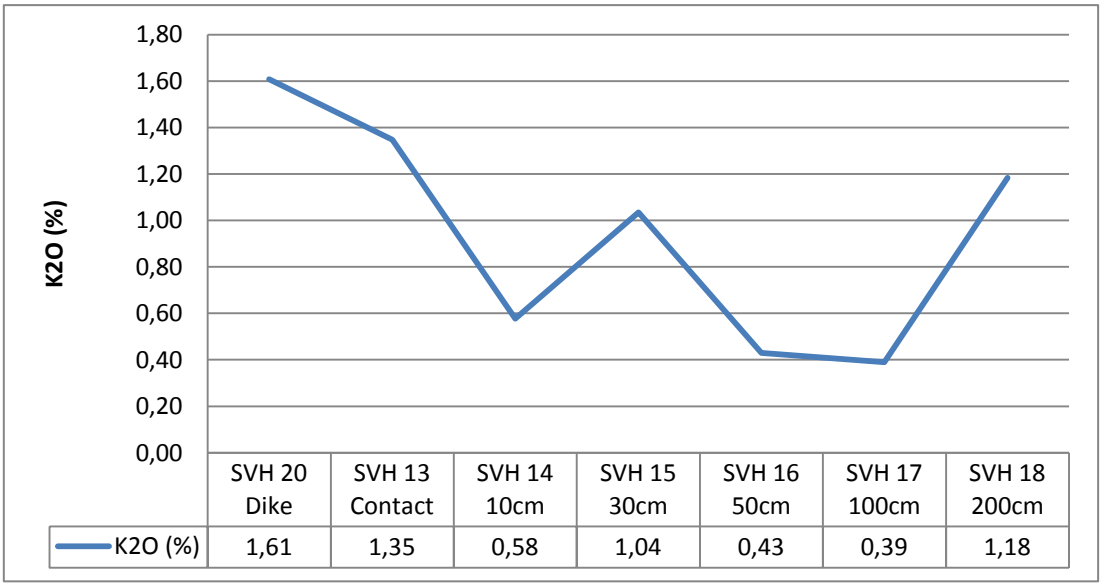

Figure 25: Graph showing the Sodium content based on the position relative to the dike

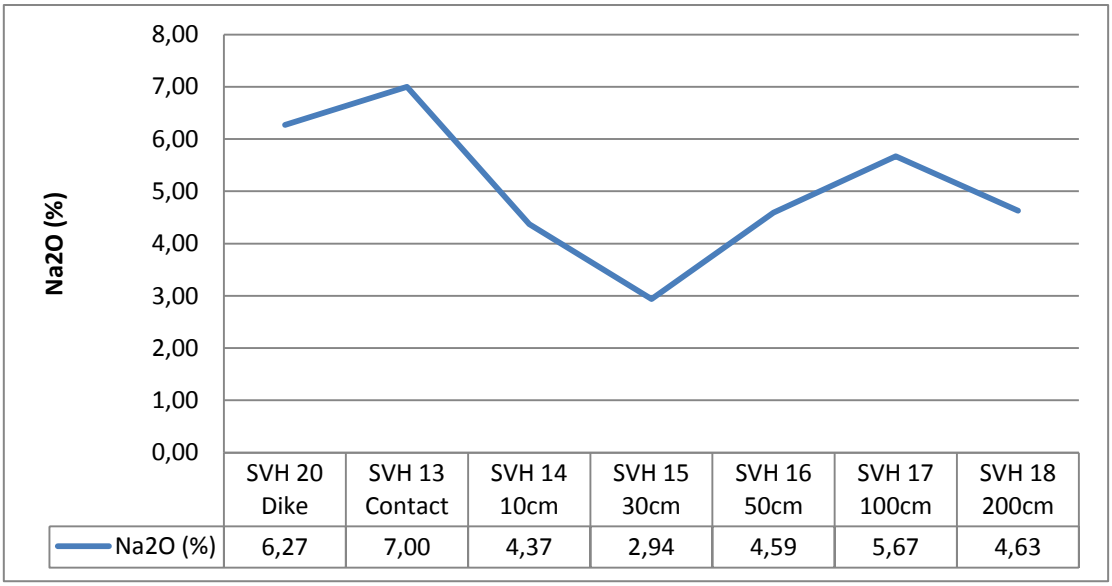

Figure 26: Graph showing the Potassium content based on the position relative to the dike

The results for Calcium (Figure 27a) show a smooth decreasing trend when moving away from the dike, as opposed to K_2O and Na_2O. However, if you have hydrothermal alteration, that would promote leeching of Ca near the contact and a gradual increase in abundance away from the dike, which is the opposite of the acquired result. Magnesium (Figure 27b) shows a slight decrease away from the dike, but has an anomalous value in sample SVH15. Generally, these Magnesium values would support the hypothesis of hydrothermal alteration, but the expected inverse correlation with Calcium is non-occurring.

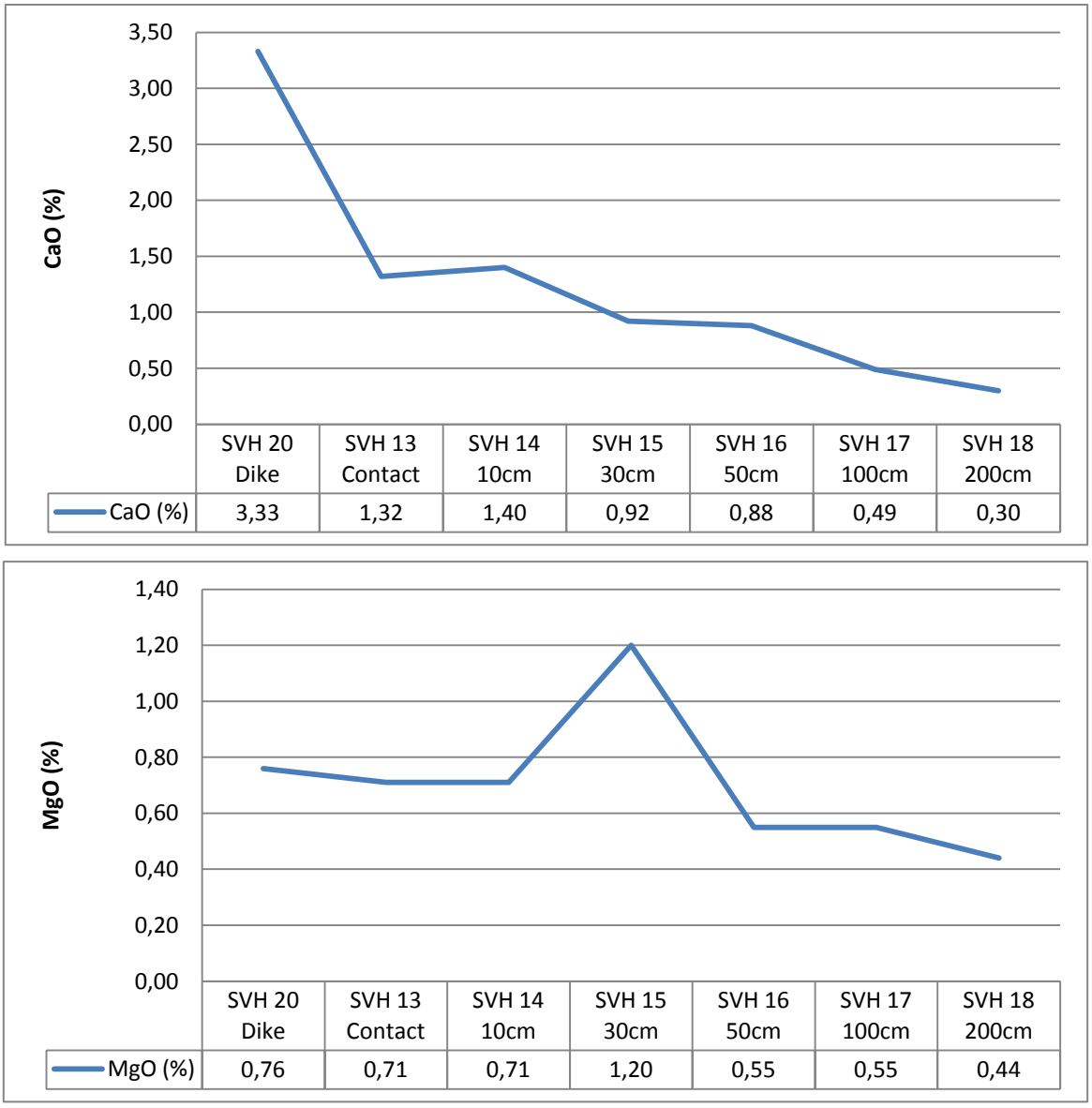

Figure 27: Graph showing the element content based on the position relative to the dike. a) Calcium. b) Magnesium.

The analyses of these elements in relation with a likely fluid conduit seem to show inconclusive results, and should not be used exclusively to decide on one or the other. According to Humphris and Thompson (1978), the Ca/Mg ratio should be close to 1 in rocks with hydrothermal alteration, due to their substituting nature. By showing the CaO+MgO as a graph (Figure 28), it becomes clear that this relationship is far from constant. Even by ignoring the value from the dike itself, there is still over 100% difference in the CaO+MgO values across this 2m interval.

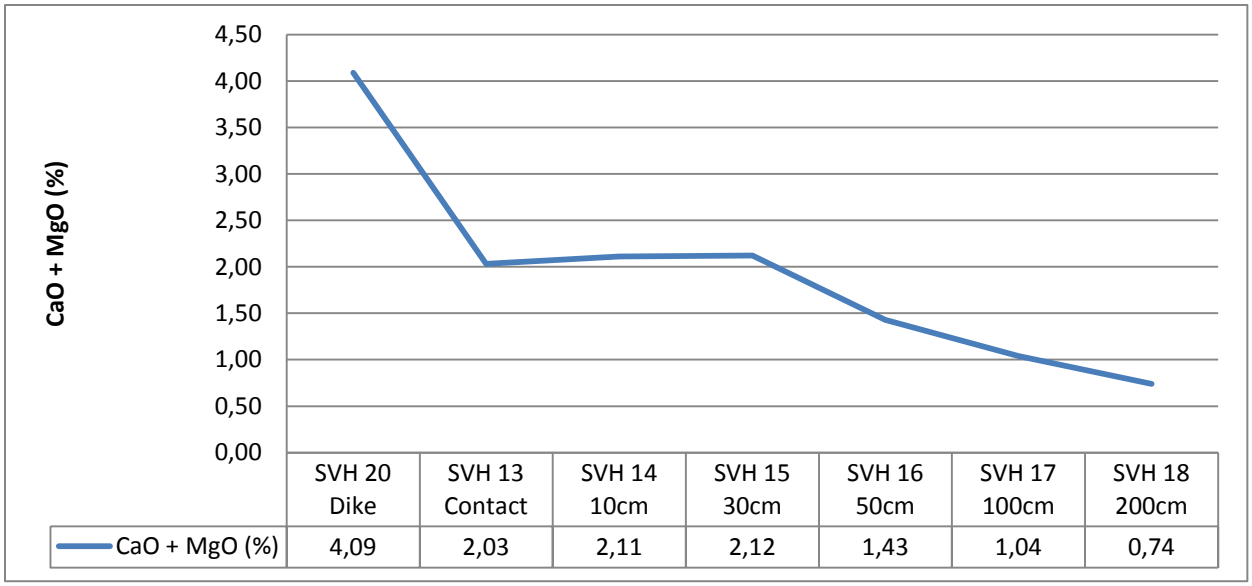

Figure 28: Graph showing the CaO+MgO content based on the position relative to the dike

The main element analyses suggest that ocean floor metamorphosis of the Klemetsaunet plagiogranite is unlikely. The trace elements seem to further strengthen this theory.

The concentration of strontium in fresh basalts usually lies between 90-190ppm. Sr is mobilized during hydrothermal alteration (Humphris and Thompson 1978), but Sr also shows an affinity towards epidote. In the sampled dike (SVH20), 527ppm Sr is recorded, which is likely due to the epidote rich nature of the dike. The Sr graph in Figure 29 shows that the Sr content indeed is enriched in the 4 samples containing epidote, while being depleted in the last 3 samples.

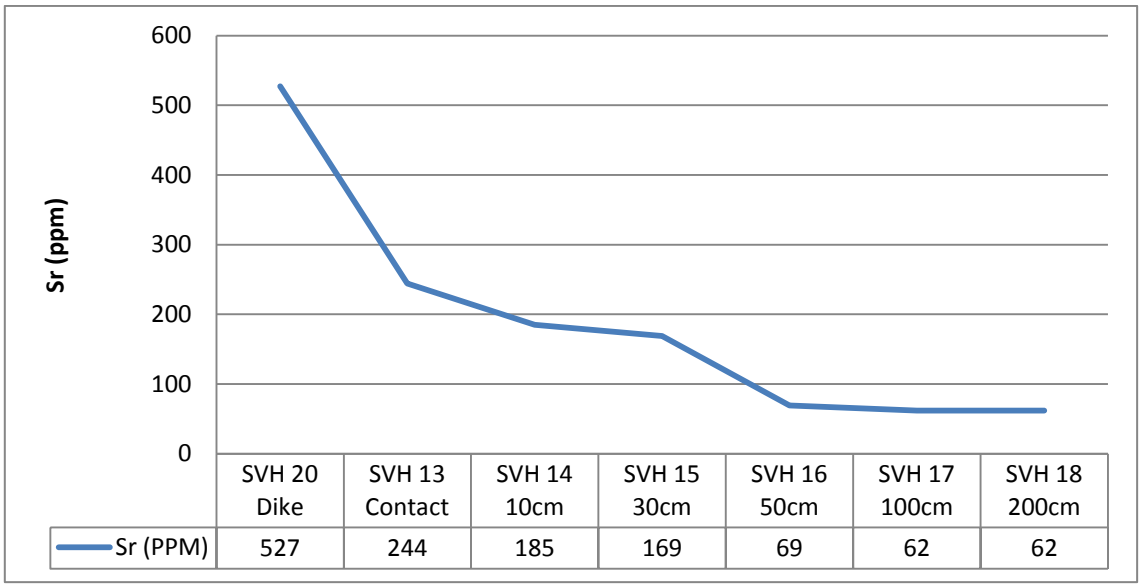

Figure 29: Graph showing the strontium content based on the position relative to the dike

For barium, fresh basalts contain <5ppm, and should see a slight enrichment in hydrothermally altered rocks (Humphris and Thompson 1978). The sampled value of Ba is 341ppm in SVH20, which is off the charts of what can be attributed to the hydrothermal alteration. This value is likely caused by a separate, non related event.

Cu, which is mobilized during hydrothermal alteration (Humphris and Thompson 1978), shows a very anomalous graph (Figure 30) when related to the distance to the dike. The big spike in this graph can be disregarded due to increased amount of sulphides in this sample. Taking this into account, the graph still shows no enrichment away from the dike, which would be expected with hydrothermal alteration.

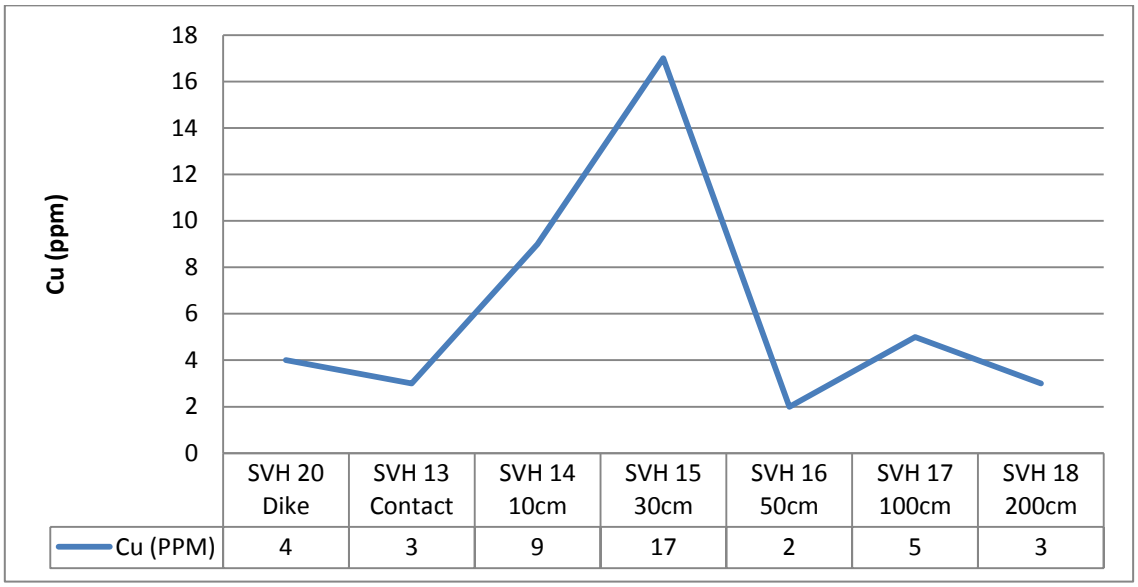

Figure 30: Graph showing the copper content based on the position relative to the dike

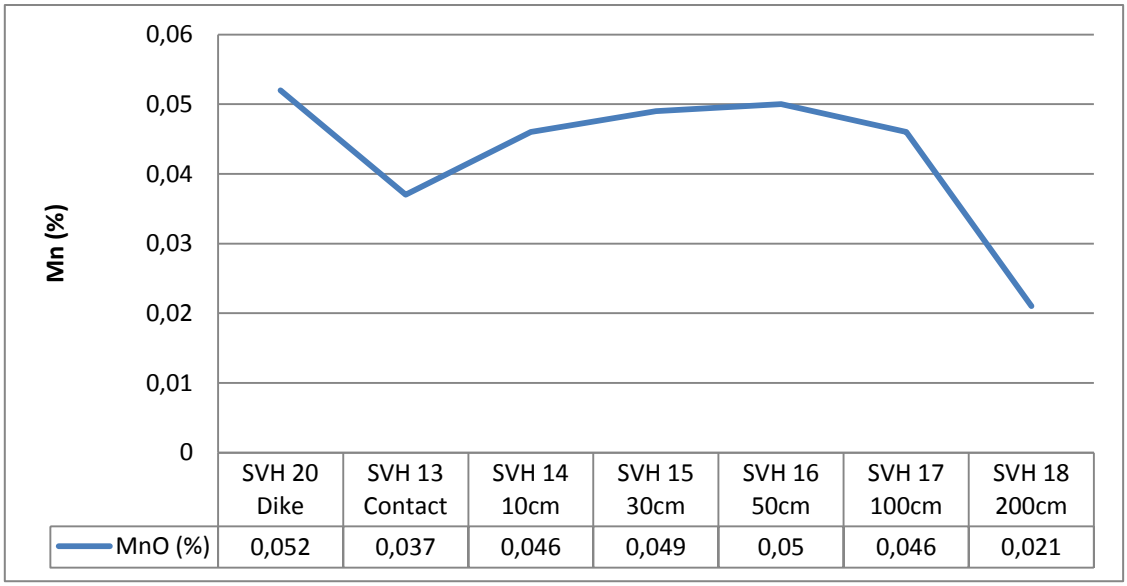

Figure 31: Graph showing the manganese content based on the position relative to the dike

A similar conclusion can be drawn from the Mn graph (Figure 31). According to Humphris and Thompson (1978), Mn is mobilized during alteration, and should show a depletion towards the dike. Meanwhile, the graph shows quite the opposite.

So, while the evidence is somewhat ambiguous, there is no consistent indication that the Klemetsaunet rocks have undergone ocean floor metamorphism. While there might have occurred some hydrothermal alteration in the area, this might have another source than sea water. Oceanic magmas contain some H_2O (Honnorez 2003), and minor hydrothermal processes may have this as a source.

6 Conclusion

A lithological map sketch of the Klemetsaunet plagiogranite and its penetrating dike is made for the field area, to supplement the less detailed existing maps.

There is no conclusive evidence supporting that the rocks at Klemetsaunet have undergone ocean floor metamorphism. Different elements that have characteristic affinities when exposed to hydrothermal alteration show diverging results from chemical analysis, making it tough to believe that ocean floor metamorphism is the dominating metamorphic process that has altered the geochemistry of the rocks in question.

Following this, it is reasonable to believe that the present day geochemistry and mineralogy of the rocks at Klemetsaunet are a result of the regional metamorphosis related to the Caledonian orogeny.

7 References

Coish, R. A. (1977). "Ocean-Floor Metamorphism in Betts Cove Ophiolite, Newfoundland." Contributions to Mineralogy and Petrology **60**(3): 255-270.

Ferrill, D. A., et al. (2004). "Calcite twin morphology: a low-temperature deformation geothermometer." Journal of Structural Geology **26**(8): 1521-1529.

Fossen, H. (2010). Structural Geology, Cambridge University Press.

Gerlach, D. C., et al. (1981). "Petrology and Geochemistry of Plagiogranite in the Canyon Mountain Ophiolite, Oregon." Contributions to Mineralogy and Petrology **77**(1): 82-92.

GoogleEarth (2012). "Google Earth." Retrieved 14.10, 2013, from http://www.google.com/earth/explore/products/plugin.html.

Grimes, C. B., et al. (2013). "Perspectives on the origin of plagiogranite in ophiolites from oxygen isotopes in zircon." Lithos **179**(0): 48-66.

Honnorez, J. (2003). "Hydrothermal alteration vs. ocean-floor metamorphism. A comparison between two case histories: the TAG hydrothermal mound (Mid-Atlantic Ridge) vs. DSDP/ODP Hole 504B (Equatorial East Pacific)." Comptes Rendus Geoscience **335**(10-11): 781-824.

Humphris, S. E. and G. Thompson (1978). "Hydrothermal alteration of oceanic basalts by seawater." Geochimica Et Cosmochimica Acta **42**(1): 107-125.

Humphris, S. E. and G. Thompson (1978). "Trace element mobility during hydrothermal alteration of oceanic basalts." Geochimica Et Cosmochimica Acta **42**(1): 127-136.

Lecuyer, C., et al. (1990). "Elemental Fluxes during Hydrothermal Alteration of the Trinity Ophiolite (California, USA) by Seawater." Chemical Geology **89**(1-2): 87-115.

Miyashiro, A. (1972). "Pressure and Temperature Conditions and Tectonic Significance of Regional and Ocean-Floor Metamorphism." Tectonophysics **13**(1-4): 141-&.

NorgeiBilder (2011). "Norge i Bilder." Retrieved 14.10, 2013, from http://norgeibilder.no/?zoom=16&lat=7036635.95117&lon=562142.57813&srs=EPSG:32632.

Ramberg, I. B. (2008). The Making of a Land: Geology of Norway, Geological Society Publishing House.

Roberts, D., et al. (2002). "U-Pb zircon ages from the Bymarka ophiolite, near Trondheim, Central Norwegian Caleclonicles, and regional implications." Norwegian Journal of Geology **82**(1): 19-30.

Robinson, P., et al. (2012). "A major synmetamorphic early Devonian thrust and extensional fault system in the mid-Norway Caledonides: Key to exhumation of HP and UHP rocks." 47.

Schermerhorn, L. J. G. (1973). "What is keratophyre?" Lithos **6**(1): 1-11.

Slagstad, T. (2003). "Geochemistry of trondhjemites and mafic rocks in the Bymarka ophiolite fragment, Trondheim, Norway: Petrogenesis and tectonic implications." Norwegian Journal of Geology **83**(3): 167-185.

Solli, A., et al. (2003). Trondheim. Berggrunnskart; 1:50 000; Foreløpig utgave, NGU**:** 1.

Streckeisen, A. (1980). "Classification and nomenclature of volcanic rocks, lamprophyres, carbonatites and melilitic rocks IUGS Subcommission on the Systematics of Igneous Rocks." Geologische Rundschau **69**(1): 194-207.

TrondheimKommune (2013). "Trondheim Kommune kart." Retrieved 10.11, 2013, from http://kart5.nois.no/trondheim/Content/Main.asp?layout=trondheim&time=1384553065&vwr=&MapType=png.

Winter, J. D. N. (2010). An Introduction to Igneous and Metamorphic Petrology, Prentice Hall PTR.

Appendix

A XRD results and interpretation:

130106: SVH1

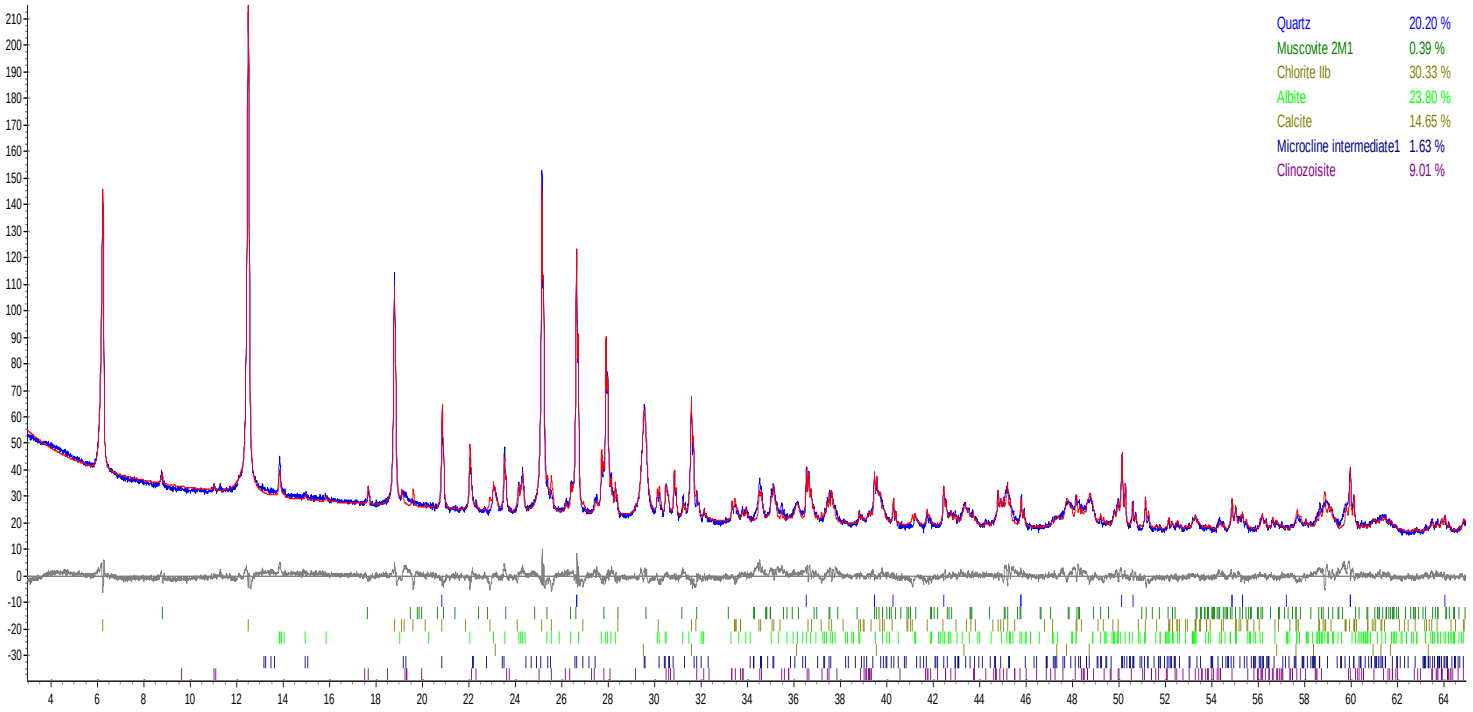

130107: SVH2

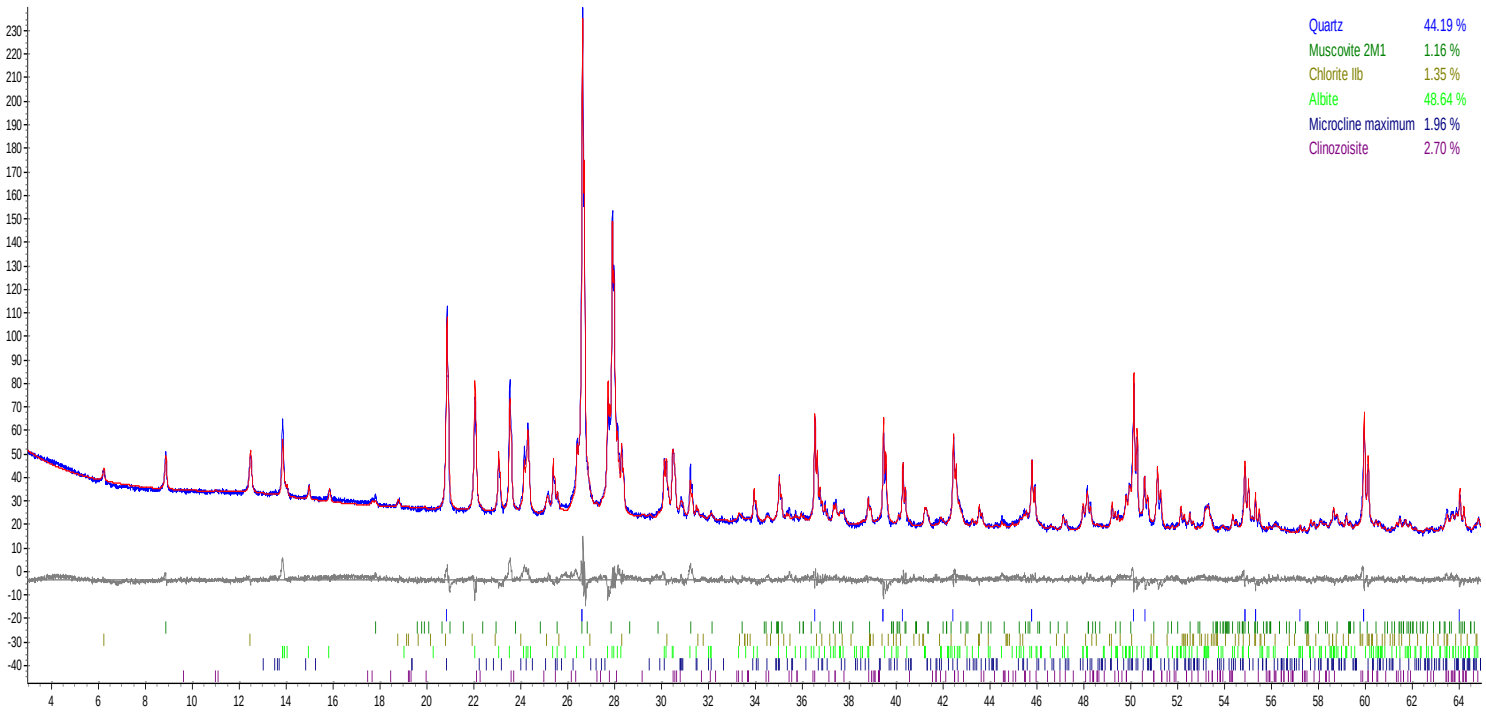

130108: SVH5

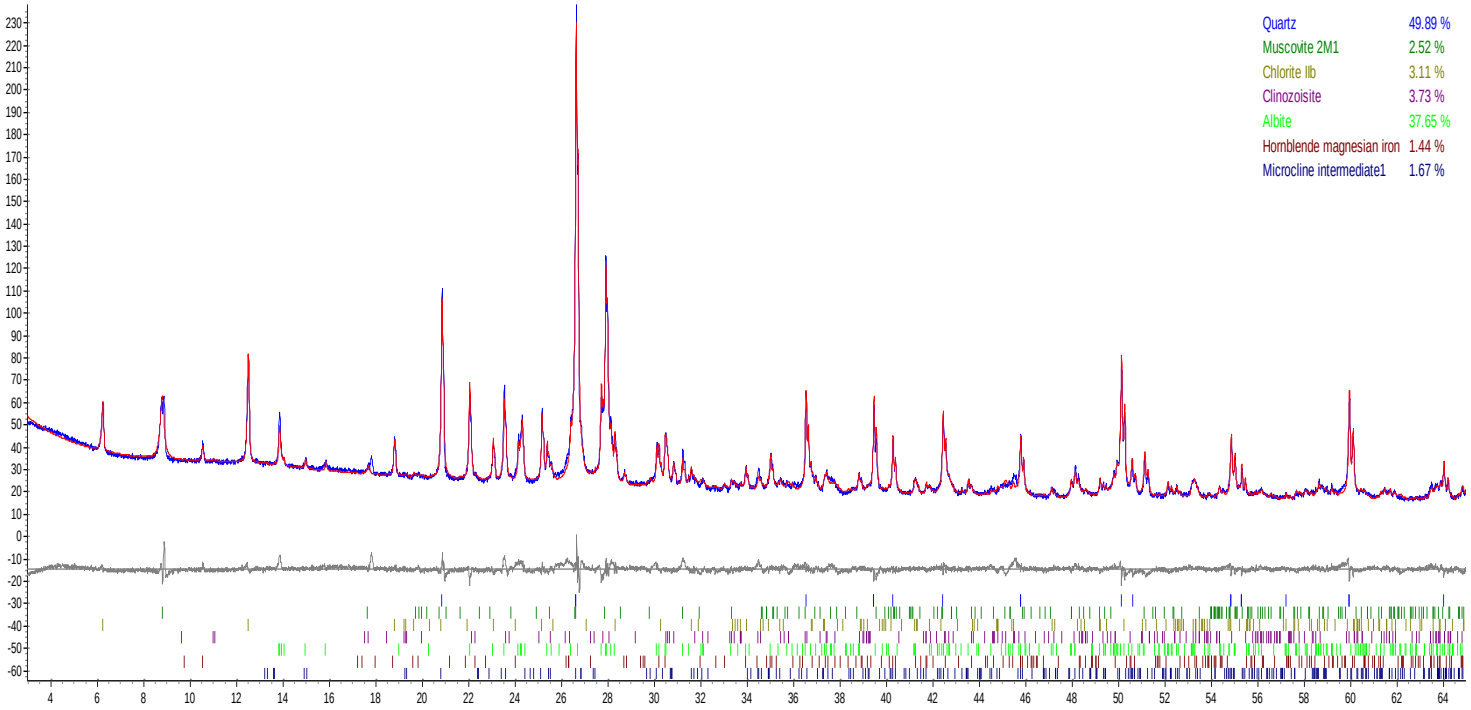

130109: SVH6

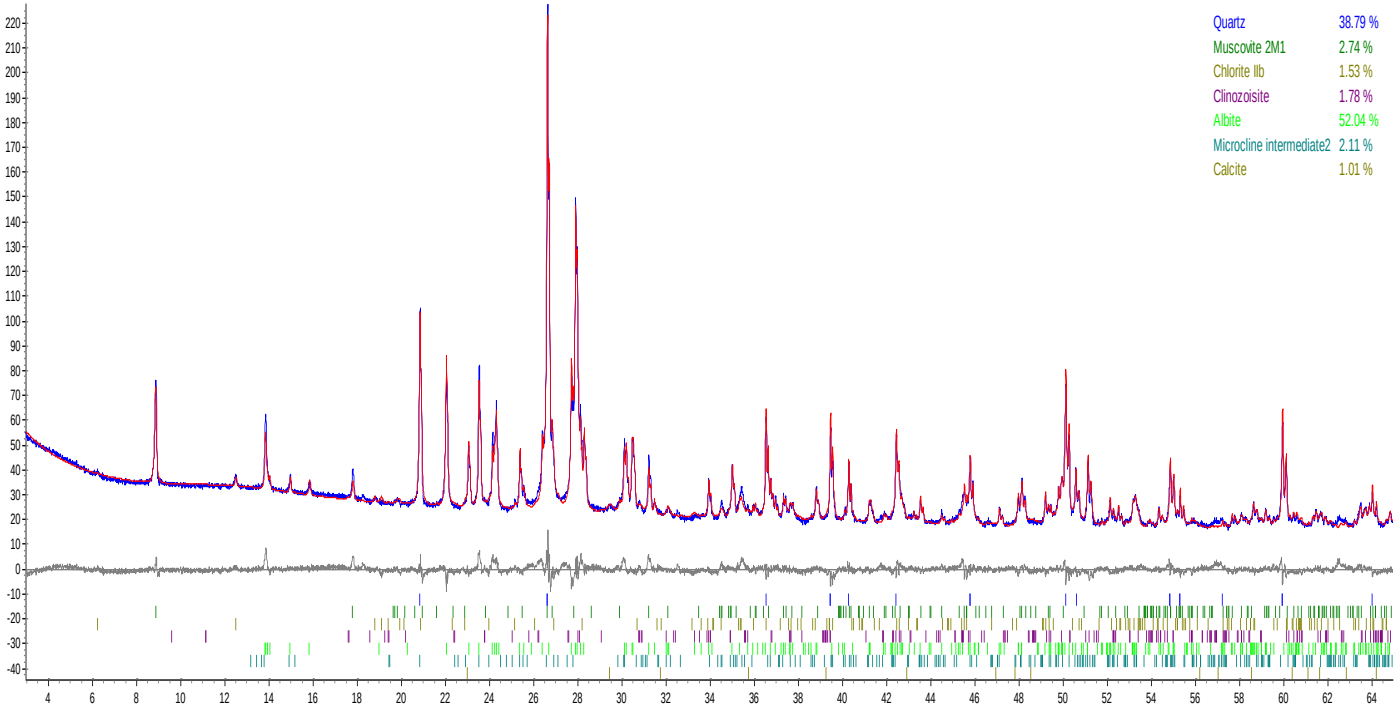

Calcite bør sjekkes med saltsyre, tynnslip

130110: SVH8

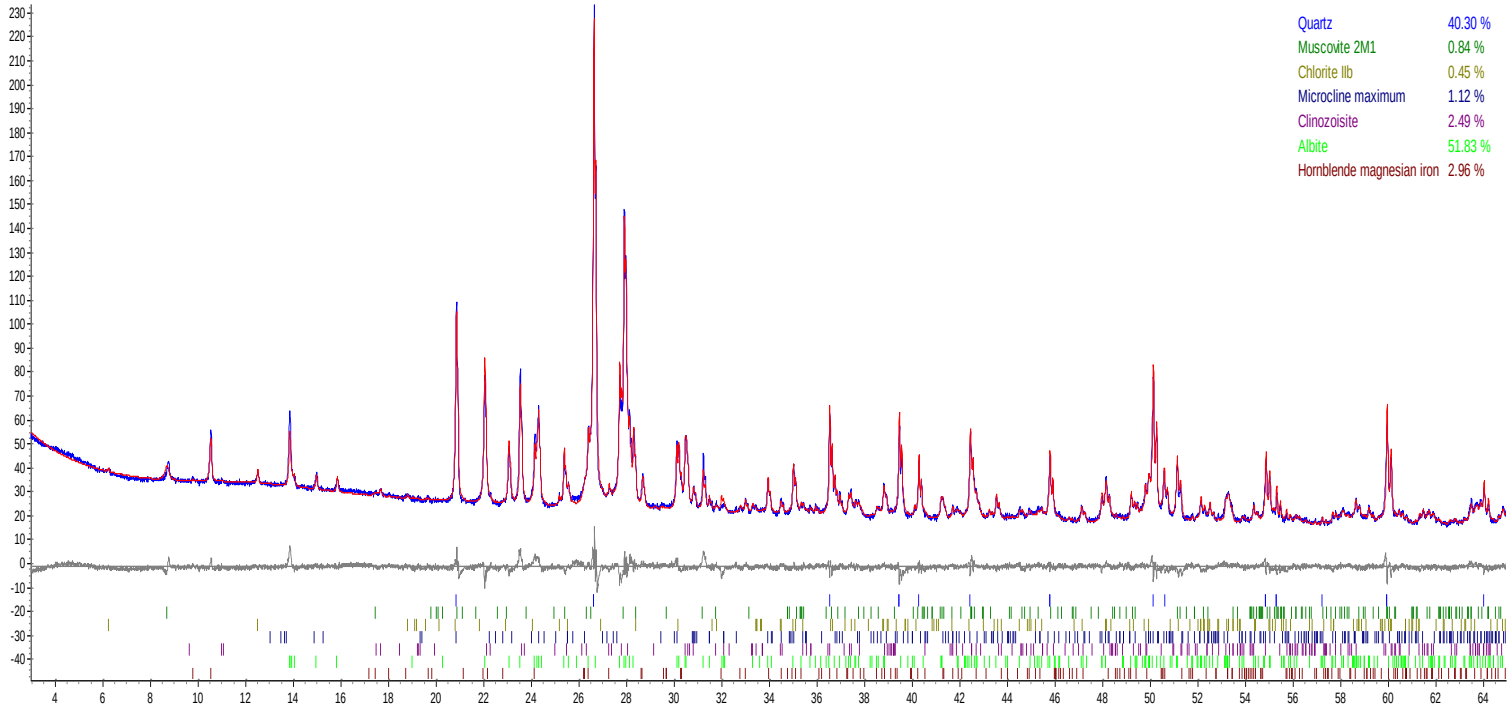

130111: SVH9

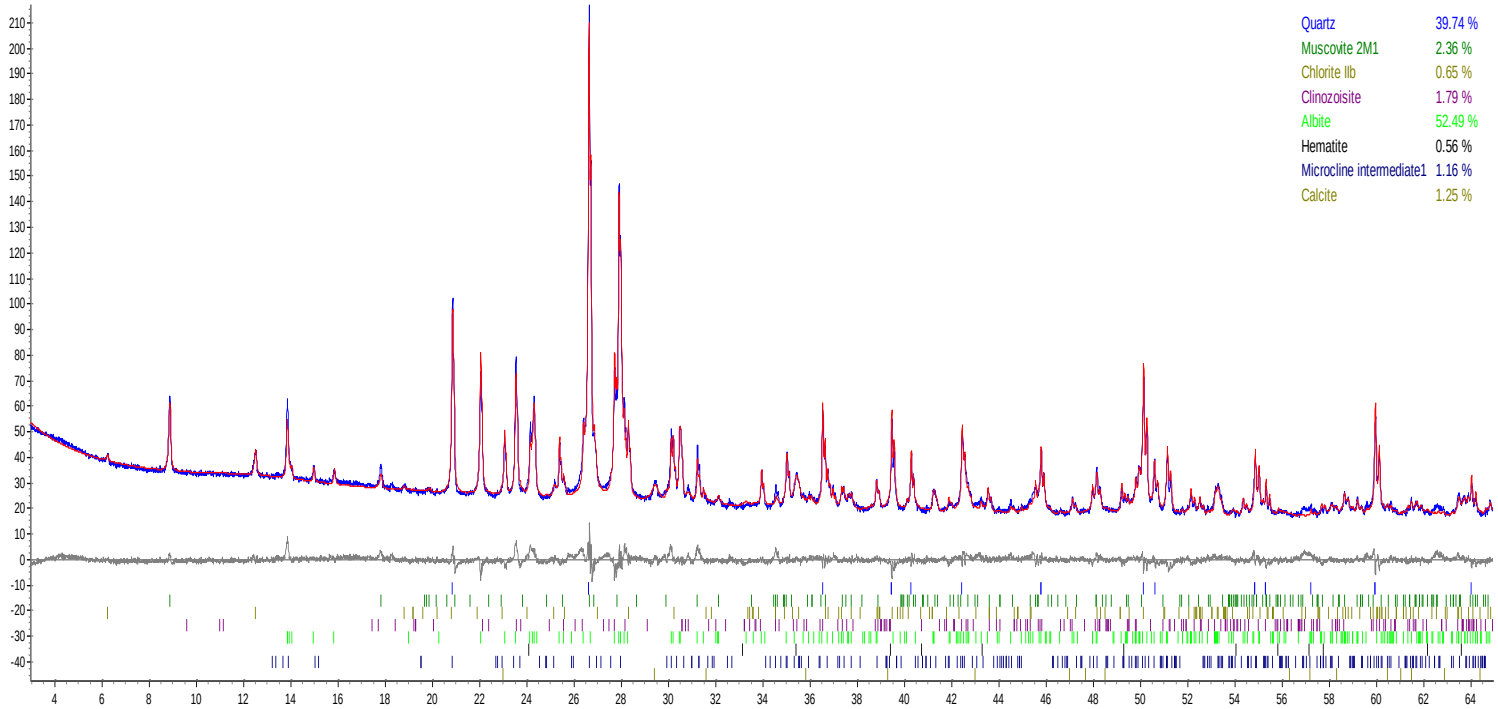

130112: SVH10

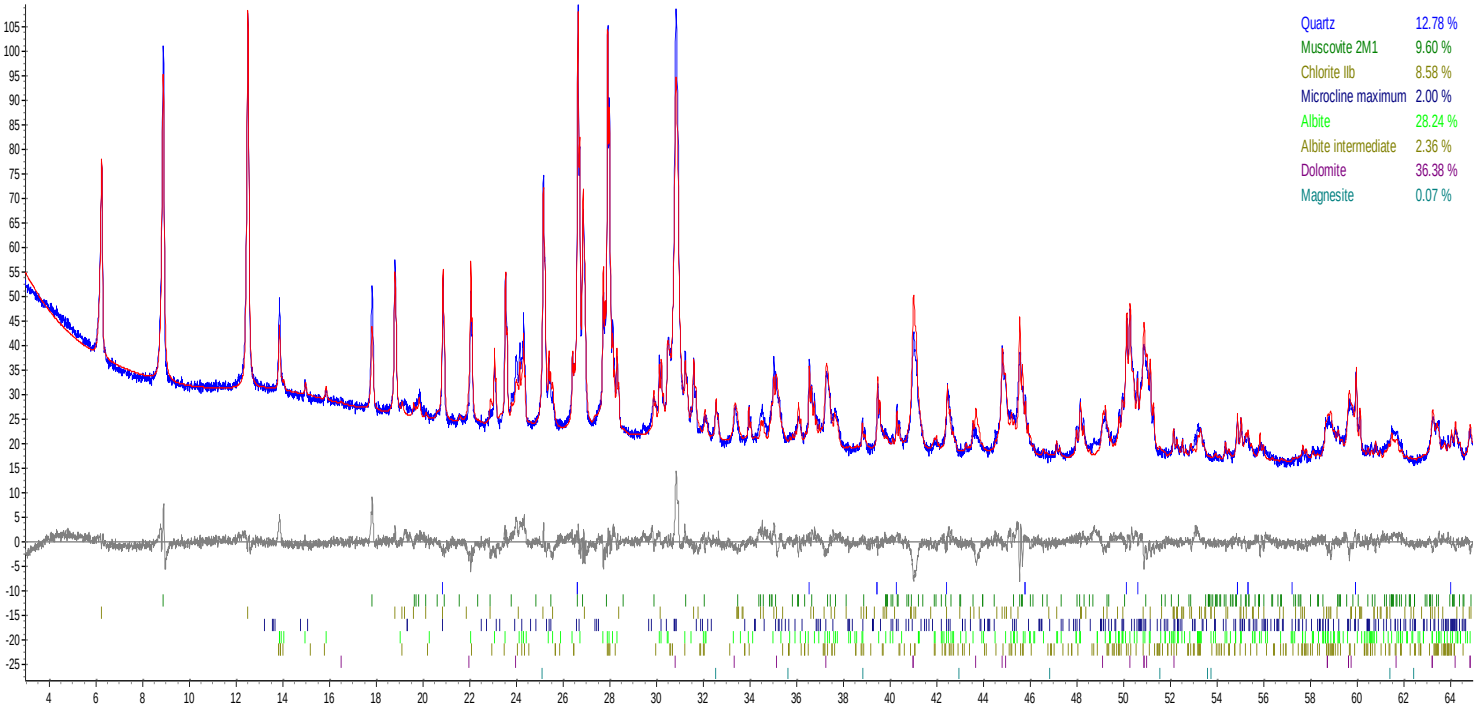

130113: SVH11

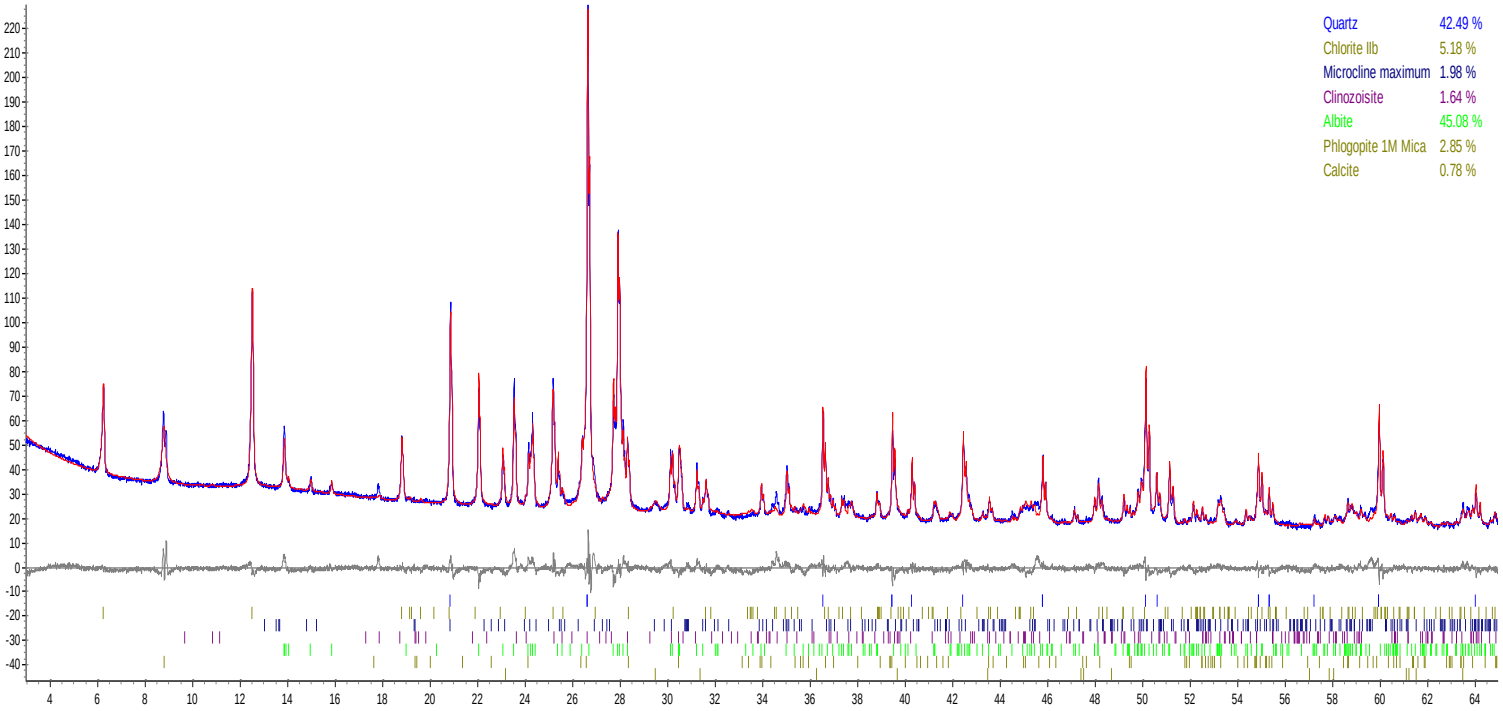

130507: SVH 13

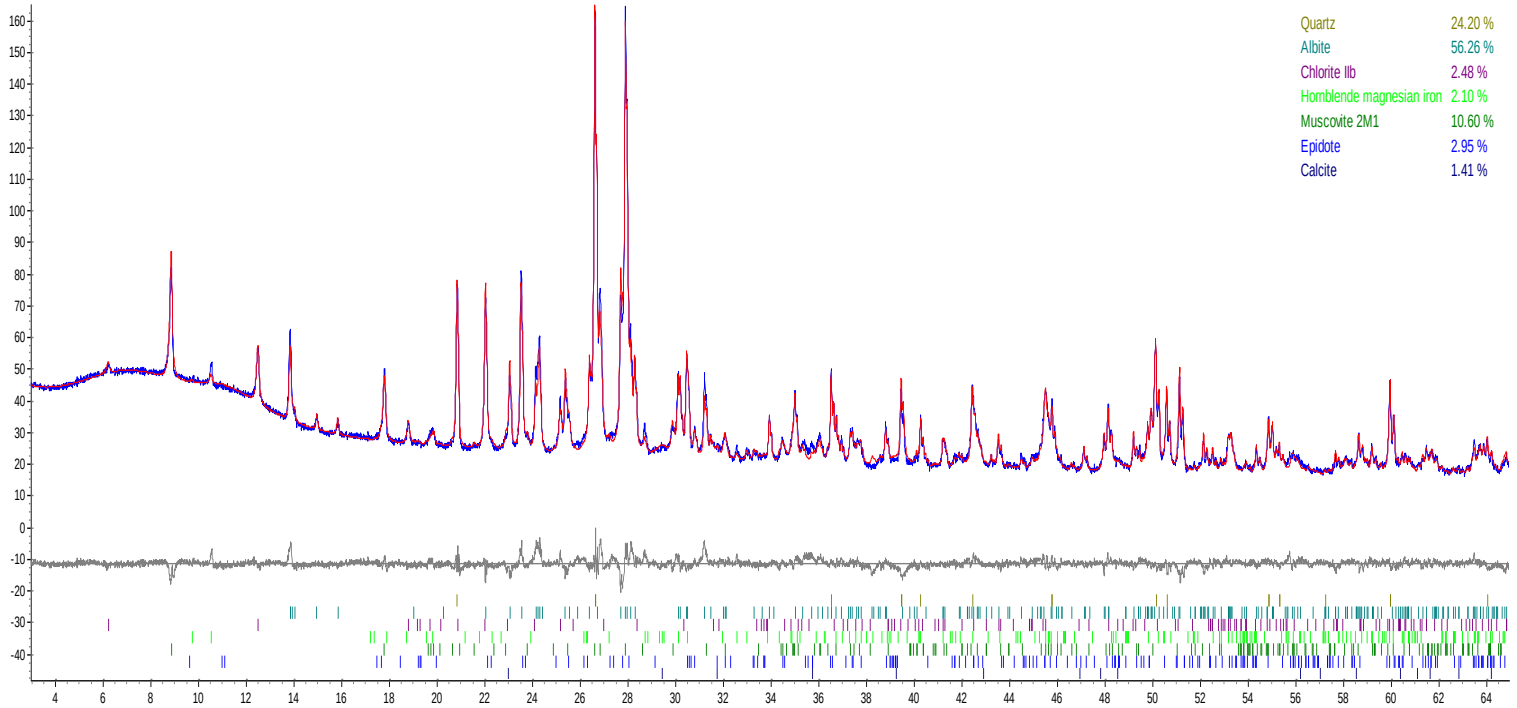

130508: SVH 14

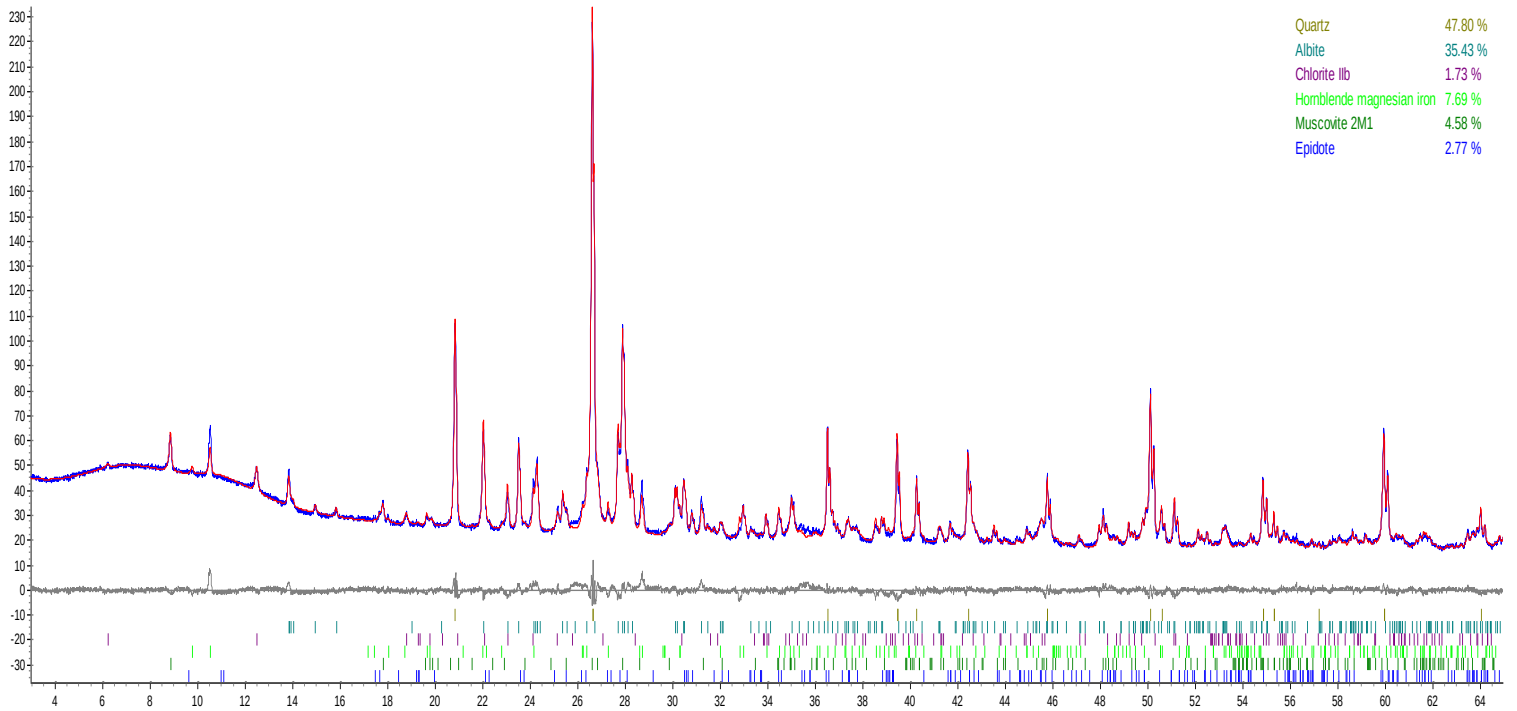

130509: SVH 15

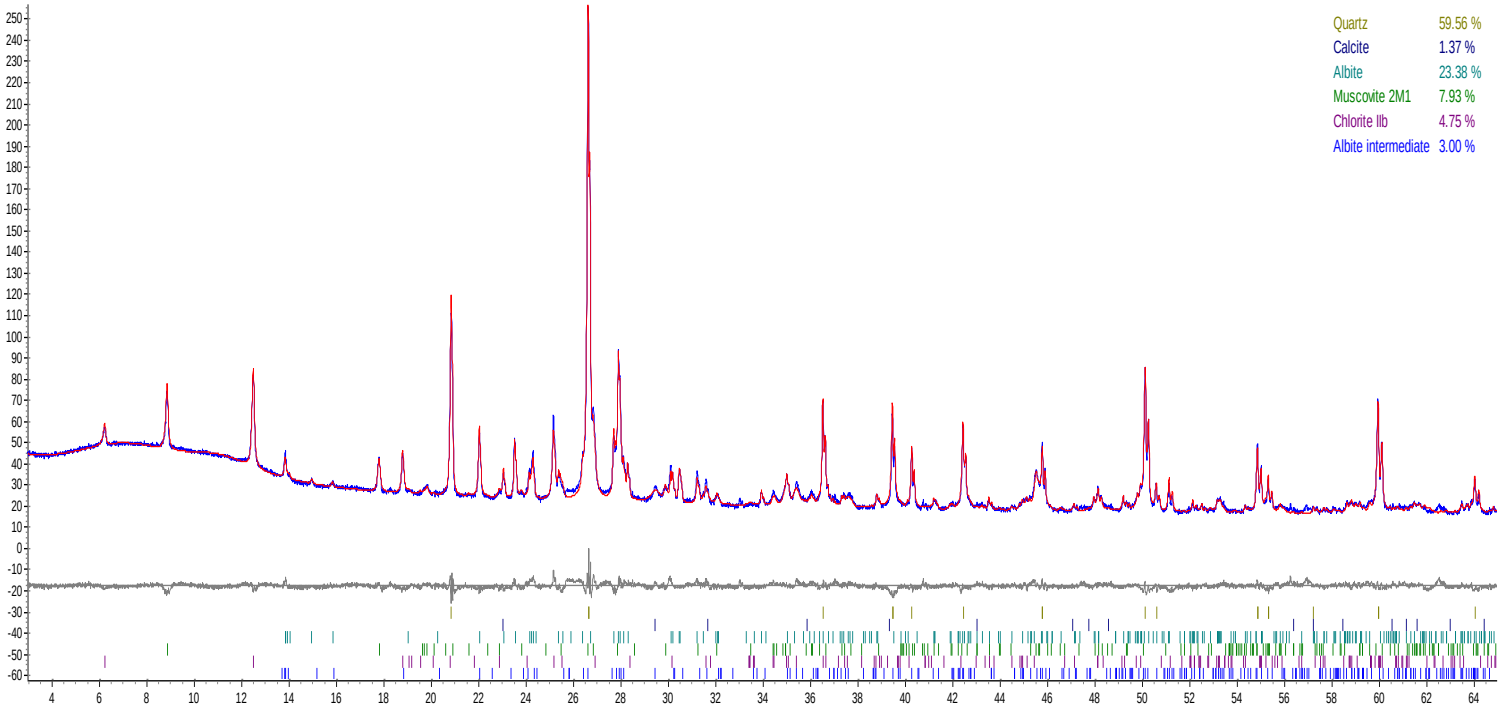

130510: SVH 16

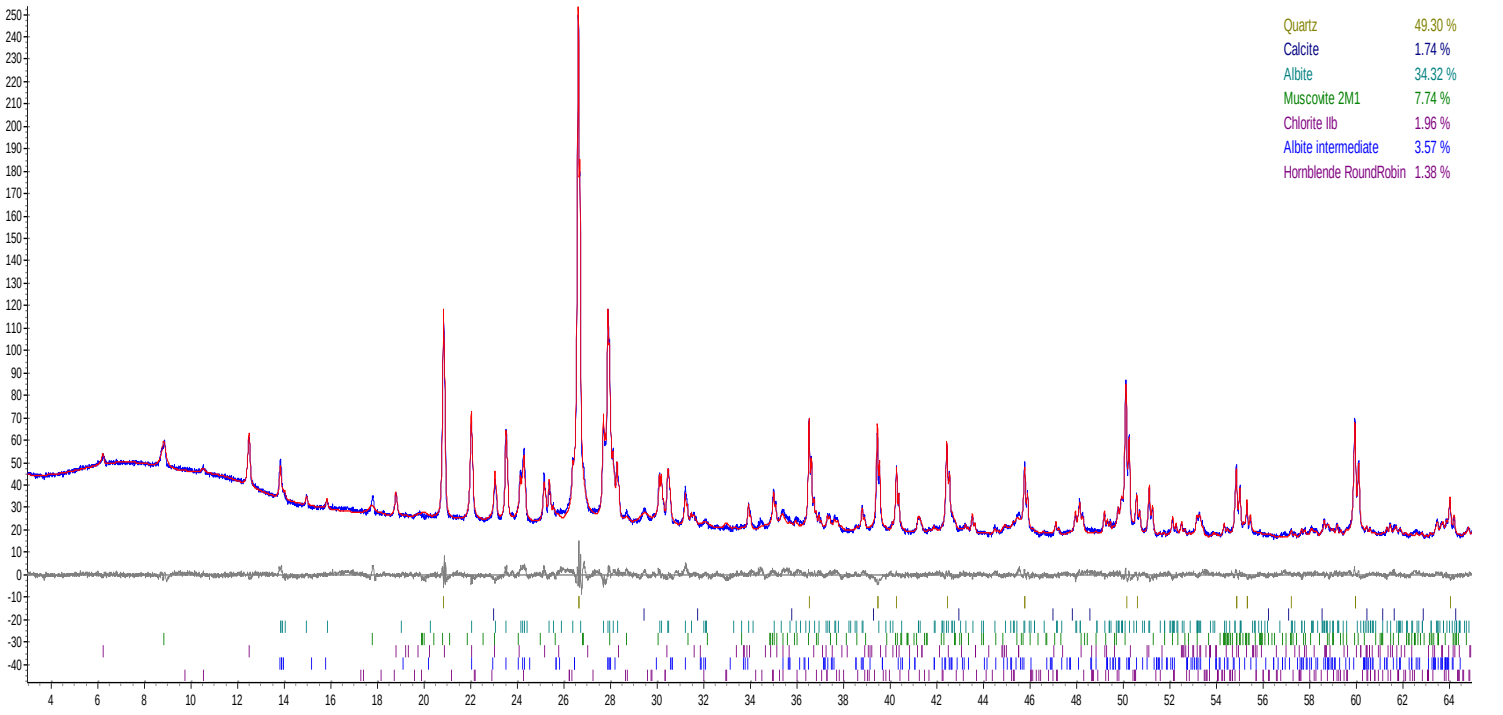

130511: SVH 17

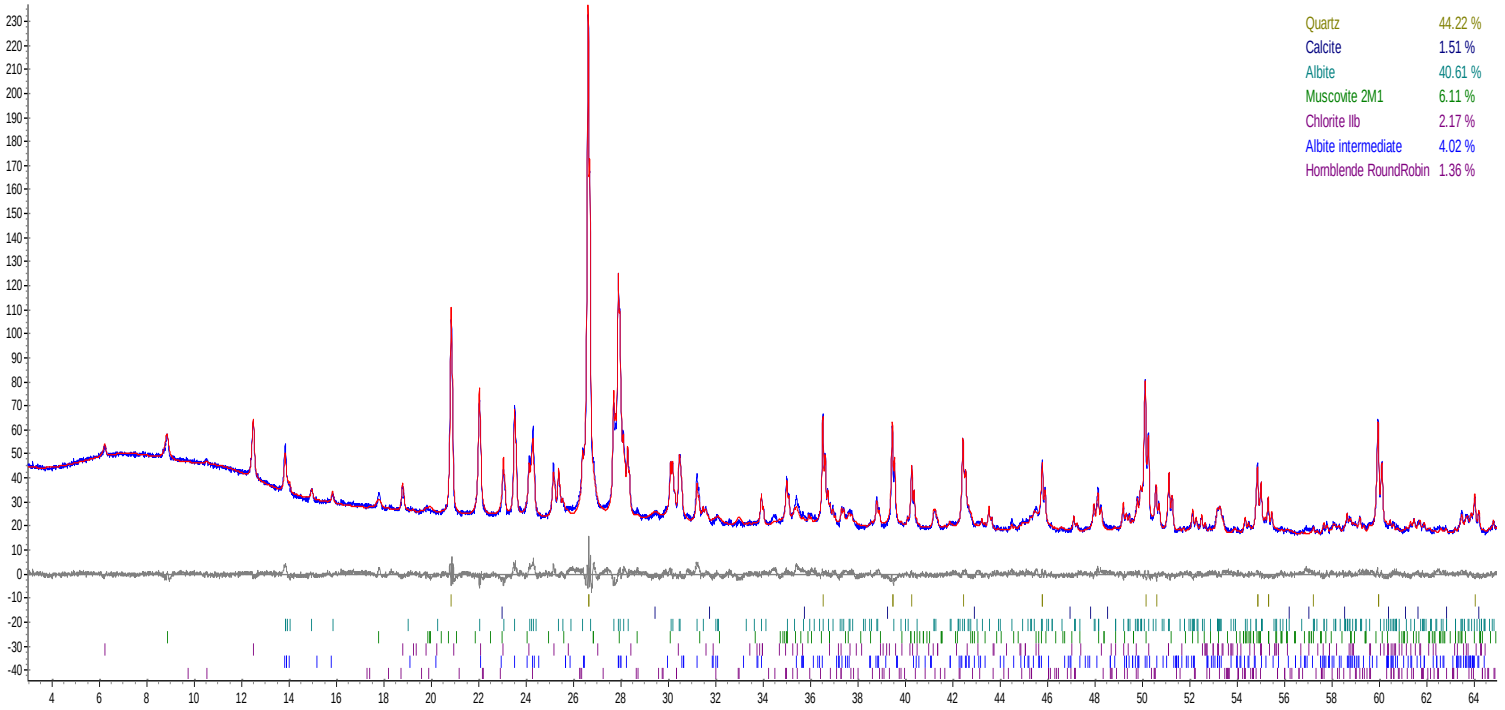

130512: SVH 18

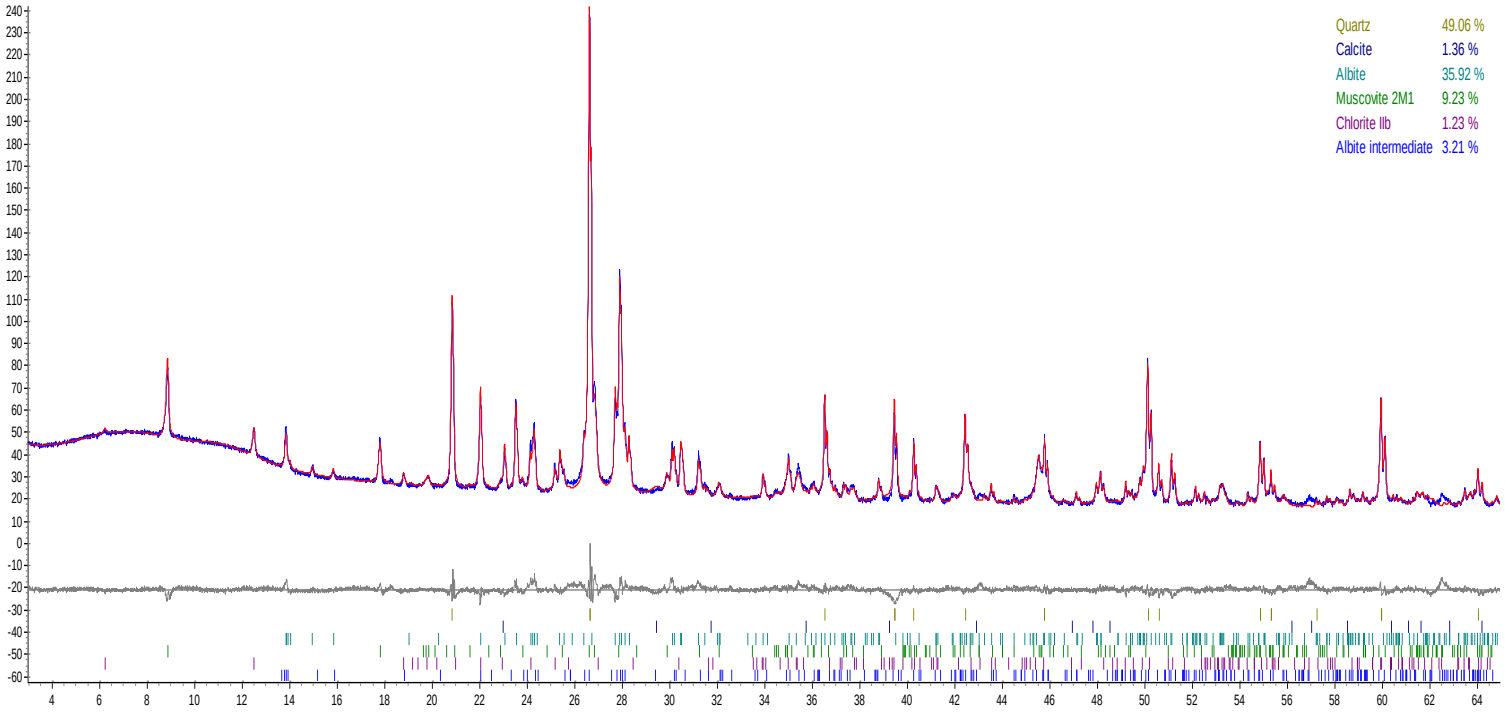

130513: SVH 19

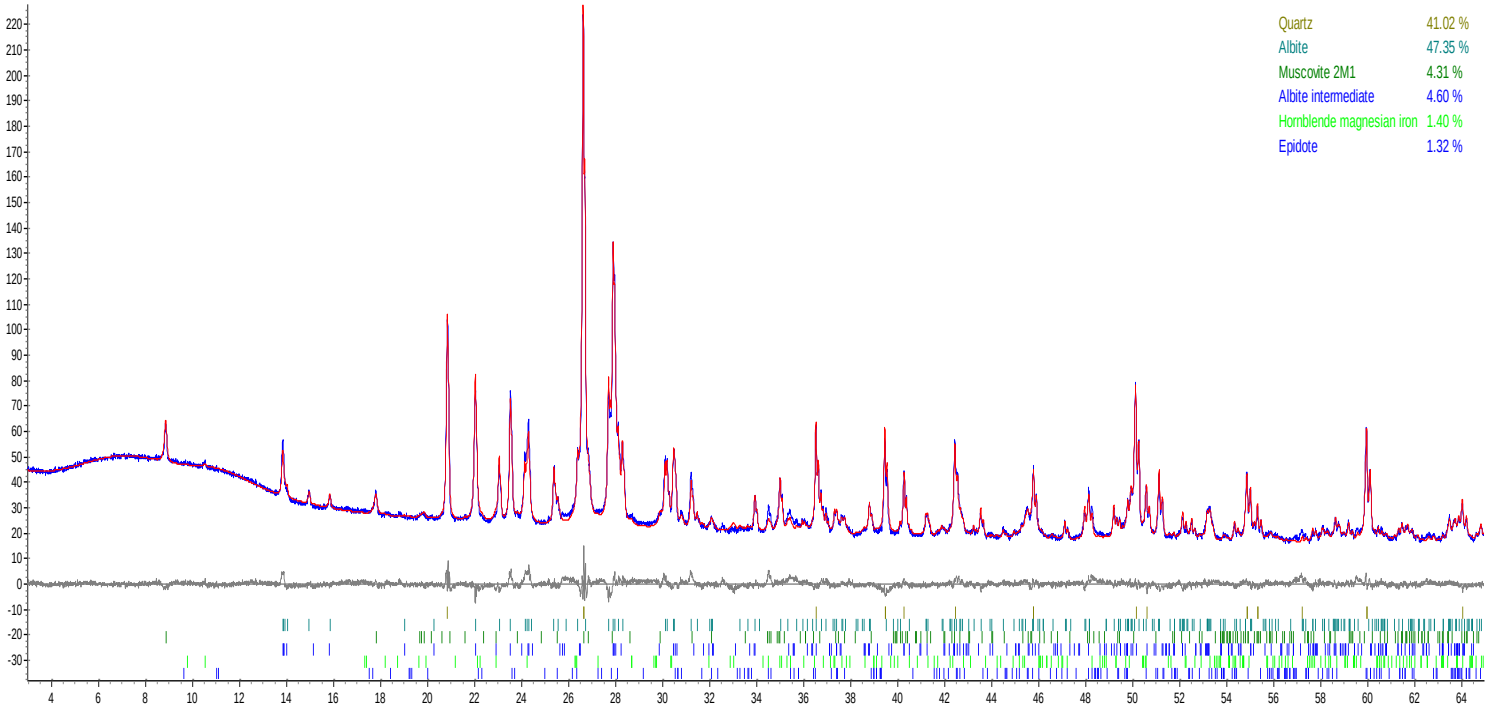

130514: SVH 20